Process Biochemistry 130 (2023) 386–400

https://doi.org/10.1016/j.procbio.2023.04.028

Received 17 February 2023; Received in revised form 21 April 2023; Accepted 25 April 2023

Available online 26 April 2023

Wax esters from waste fish oil catalysed by immobilized Candida rugosa lipase

Mariagrazia Iuliano a,1,*, Eleonora Ponticorvo b,c,1, Claudia Cirillo b,c,1, Rachele Castaldo d, Salvatore De Pasquale b, Gennaro Gentile d, Maria Sarno b,c

a Department of Industrial Engineering, University of Salerno, via Giovanni Paolo II, 132, 84084 Fisciano, SA, Italy

b Department of Physics "E.R. Caianiello" University of Salerno, Via Giovanni Paolo II, 132, 84084 Fisciano, SA, Italy

c NanoMates, Research Centre for Nanomaterials and Nanotechnology at the University of Salerno, University of Salerno, Via Giovanni Paolo II, 132, 84084 Fisciano,

SA, Italy

d Institute for Polymers, Composites, and Biomaterials, National Research Council of Italy, Via Campi Flegrei 34, 80078 Pozzuoli, Italy

Keywords: Waste fish oil Magnetic support; Amino-hyper cross-linked resin; Emollient ester; Synthesis; Transesterification reaction

ABSTRACT

Herein, the evaluation of waste fish (WF) oils as feedstock for the production of wax esters through trans-esterification reactions was reported. In particular, the synthesis of an emollient ester in the presence of oleyl alcohol and using an immobilized lipase catalyst was proposed. Lipase from Candida rugosa (CRL) was immo- bilized (0.5 enzyme/support wt. ratio) on a magnetic amino-functionalized hypercross-linked resin (M-HCLR- NH2) by ion exchange, interfacial activation, and covalent anchoring, mediated by 1-ethyl-3-(3-dimethyl-amino- propyl)carbodiimide (EDC). The experimental results demonstrated the successful immobilization of lipase on the as-produced M-HCLR-NH2 with a high immobilization yield of 90%. The immobilized CRL showed very high activity and an activity recovery of ~ 94%. The immobilized enzyme on the magnetic resin results in more stability and less sensitivity to temperature change than the free counterpart. In addition, during emollient ester synthesis in a solvent system, the immobilized enzyme exhibited very high activity, stability, and excellent reusability, with a yield of 94% after 12 h at 45 ◦C at an oil:alcohol molar ratio of 1:4 and an immobilized enzyme concentration of 15 wt%./wt of oil. Esters synthesized showed excellent physicochemical properties.

1. Introduction

Wax esters are long-chain esters that are derived from fatty acids and fatty alcohols with more than 12 carbon atoms. They show no toxicity [1] and are classified as fine chemical products [2]. The wax esters global market had a size of 10.2 billion dollars in 2022 and is expected to register a growth rate of ≈ 3% by 2027 [3]. They have wide applications in the production of candles [4,5], printing inks [6], rubber, coatings [7], and lubricants [4]. Wax esters can be used to produce pharmaceu- ticals [6] and personal care products [8], such as emollients [8,9], cosmetics [6], skin care [10], hair care [10], and others [11]. Wax esters can be obtained from natural sources or chemical synthesis, e.g., from petroleum. Natural sources, from which to extract the fat components, or oils directly, can be used to derive wax esters with different compo- sitions [12]. Jojoba oil has been the first natural source for wax ester synthesis [13]. However, costs and availability hinder the large-scale application of oil from jojoba. For this reason, attempts to synthesize wax esters [14] with cheaper raw materials in a shorter time are issues of great significance. Among the different possibilities, the use of cheaper vegetable oils is a very significant option as an alternative to natural wax ester sources. Due to competition with food crops, edible oils are not a feasible option. On the other hand, the valorization of wastes and biomasses is a valid and promising alternative to obtaining wax esters. Currently, the fish processing industry is one of the most important in the world. During fish processing operations, a significant amount of fish byproducts are generated as waste in the form of viscera, frame head skin scales, etc.[15]. A certain part of these wastes is utilized as low-cost ingredients in animal feed production and fertilizer. Instead, the main bulk of these wastes is considered valueless garbage, resulting in disposal costs, while their inadequate disposal creates pollution prob- lems [15,16]. It is worth noting that some of these wastes contain a high amount of oil. Typically, fishes contain 2–35 wt% fat, while approxi- mately 50 wt% of the body weight is generated as waste during fish processing operations [15]. Omega-3 fatty acids, which are abundant in fish oil, are involved in different physiological activities as essential fatty acids. They exhibit an important role in the body's homeostatic pres- ervation. In particular, omega 3- polyunsaturated fatty acids (PUFAs), such as docosahexaenoic acids (C22:6n-3) and omega-3 eicosapentae- noic (C20:5n-3), possess health benefits. However, ~15–22% of omega-3 fatty acids in waste fish oil are useless. Extracted waste fish oil may not meet the quality criteria required for edible purposes. Furthermore, in the presence of highly polyunsaturated fatty acids, fish oils exhibit highly unpleasant flavours and odours. On the other hand, wastes from fish have been used to produce biodiesel [17–21] and esters [22–24]. In addition, by the disposal of fish, other high-added-value products, such as peptides, have also been produced [25–27].

Transesterification/esterification [28,29] reactions can be used for the synthesis of wax esters from vegetable oils or fats with alcohols in the presence of a chemical homogeneous or heterogeneous catalyst. Ester- ification, which shifts the reaction equilibrium towards ester production with the addition of excess reagents or removal of formed catalytic unnecessary water molecules, is a thermodynamically controlled pro- cess [30]. However, transesterification is a kinetically controlled reac- tion [31]. In particular, chemical catalysts, although active and selective [32], present several disadvantages, such as (i) high reaction tempera- tures, (ii) difficulties in separation from the reaction media, (iii) low yields, and (iv) environmental concerns [33]. On the other hand, bio- logical reactions involving enzymatic catalysts have been demonstrated to be attractive for the synthesis of wax esters because they are processed with low energy consumption, high productivity and selectivity, and good stability compared to organic solvents [34]. In addition, they have broad substrate specificity and exhibit high enantioselectivity [35].

The performance of an enzyme depends upon various factors, including enzyme active centre adsorption characteristics, enzyme specificity, and reaction inhibitions [36]. However, enzyme cost and process stability require, to prolong the applicability of enzymes in syntheses of wax esters or other industrial processes, the implementation of techniques allowing stabilization and reuse. Among these techniques, enzyme immobilization stands out [35–39]. To extend the applicability of enzymes in syntheses of wax esters, or in other industrial processes, the implementation of techniques allowing stabilization and reuse are needed.

Several methods are used for enzyme immobilization [40,41]. Among them, the most commonly used are based on physical and chemical immobilization (covalent bonds) [42–44]. In particular, covalent bonds, although they do not allow for the reuse of esters when enzyme inactivity occurs, ensure that the enzymes are strongly bound to the support, preventing the mixing of the enzyme with the products, thereby reducing contamination and the cost of purification [45] and favouring better stability towards organic solvents and higher temperatures. Covalent binding also stabilizes the enzyme in specific protein orientations, which may promote higher specific activity. The physical method, for which stability control is more difficult [46], is a reversible, low-cost, and quite simple method, and enzymes retain activity through relatively chemical-free enzyme binding [47]. Moreover, covalent and physical immobilization techniques have demonstrated the ability to successfully provide stable forms of enzymes [48].

Support materials play a key role in the activity of an immobilized enzyme and should be low-cost and possess an adequately large surface area together with low diffusion limitations in the transport of substrate and product. Different attractive supports, such as microspheres, chitosan beads, and porous materials, were used for the immobilization procedures. In particular, mesoporous and macropore materials have structures full of pores and a larger surface area, so they are usually applied as catalyst supports [49]. Moreover, materials with large pores can provide suitable space for the conformational conversion of the enzymes to increase their activities. For example, Miletic et al. [50] prepared macroporous poly(glycidyl methacrylate-co-ethylene glycol dimethacrylate) resins with a specific surface area of 106 m2/g and pore size distribution in the range of 50 - 560 nm to ensure immobilization of Antarctica lipase B. In recent years, hypercross-linked polymers (HCPs) have become one of the most promising carriers because of their excellent structural designability and large specific surface area [51]. Furthermore, amino functionalization of the support surface [52,53] can be useful to enhance bond strengths between enzymes and support surfaces, contrasting leaching and favouring good reproducibility and high efficiency [54,55]. However, complicated and annoying processes are needed to remove the immobilized enzyme from the reaction media. Magnetic functionalization [56] can be used to facilitate these separation processes, reducing costs and improving reusability [57], thus enhancing biocatalyst lifetime. Among magnetic nanomaterials, Fe3O4 nanoparticles (NPs) have been regarded as very promising carriers due to their biocompatibility and low cost [39,58–65]. The Fe3O4-loaded enzymes are easy to recover by a magnetic field, which may optimize operational cost and enhance product purity.

Here, for the first time, emollient esters were synthesized from waste fish oil (WF) in the presence of oleyl alcohol and Candida lipase (CRL). Although lipases have broad specificity, they are the most widely used class of enzymes in biotechnology [66], and this is for different reasons: industrial preparations of many lipases were available, given their ap- plications, in early industrial enzymology; there is a wide range of sources; they carry out reactions often in heterogeneous media showing the phenomenon of interfacial activation; and they can promote different reactions [67]. Candida rugosa lipase is an inexpensive lipolytic enzyme; moreover, it is one of the most important lipases from a com- mercial point of view. It has been used as an enzyme model due to its high applicability in biotransformations of numerous important prod- ucts [68,69], wide substrate specificity, good selectivity, and region -/- stereoselectivity [70]. Under physiological conditions, this enzyme catalyses triglyceride hydrolysis with no positional specificity. It is also stable in organic solvents and does not require any cofactors. CRL can also be utilized for catalysing esterification and transesterification re- actions. It shows wide substrate specificity for fats and oils of both vegetable and animal origins. These substrates are practically insoluble in water, so the reaction occurs at the water-lipid interface, where lipases show higher catalytic activities and interfacial activation phenomena [71], characterized by complete enzyme lid opening inducing improvement of enzymatic activity [72]. CRL was directly immobilized on an amine-functionalized high surface area support [63–65]. Among the covalent immobilization strategies, EDC can be chosen because of its robustness and minimal need for chemical modification [73,74], which has led to its extensive use in biofunctionalization for research and commercial

purposes. EDC promotes a coupling mechanism of interaction, without becoming part of the final amide bond between the target molecules.

In particular, to design a new “catalytic system”, which ensures functionalities for catalyst stabilization and allows the exploitation of enzyme selectivity, an amino-functionalized, hypercross-linked resin (HCLR-NH2) was chosen. The resin, obtained from aromatic monomers and embedding magnetic Fe3O4 nanoparticles, was used as a high sur- face area support for multiple interactions, including ion exchange, interfacial activation, and covalent immobilization, mediated by 1- ethyl-3-(3-dimethyl-aminopropyl) carbodiimide (EDC). It also works as an enzyme protection structure and alcohol cage. The immobilized enzyme was tested for activity and stability during emollient ester synthesis through transesterification reactions. Furthermore, the physico-chemical properties of the esters were evaluated.

2. Experimental design

2.1. Materials

The fish processing waste (Fig. 1) used in the current study was collected from a local fish market in Campania, Italy, and stored at -20 ◦C before use. The less valuable edible parts of fish mackerel and cod, such as heads, tails, fins, and organs, were taken as fish waste and used for the production of wax esters. CRL was acquired from Sigma Aldrich (free of protease and alpha-amylase). All chemicals used in this work were of analytical grade and acquired from Aldrich Chemical Co.

2.2. Waste fish oil (WF oil) extraction

Before extraction, 1 kg of the waste fish was thawed overnight at 8 ◦C. The material was then ground to a coarse powder. The extraction of WF oil was carried out in n-hexane. The solvent-mediated extraction method, rather than the more common method, e.g., heating with boiling water and subsequent squeezing, was used to avoid time- consuming processes and the expensive steps of filtration and drying and to obtain a drier oil with a higher yield. In particular, the milled WF, 500 g, was mixed with 1.5 l of n-hexane (1:3 w/v) and stirred for 60 min at room temperature. The mixture was then centrifuged at 7500 rpm for 30 min at 15 ◦C. The supernatants were collected, and a rotary vacuum evaporator was used for hexane removal, while the residue of extraction was reused to obtain a high- recovery oil. The following equation (Eq. 1) was used to evaluate the extracted oil [75]:

$$\text{Oil}(\%) = \frac{(\text{wt.of extracted oil})}{(\text{wt.of waste fish})} * 100 \qquad (1)$$

where “wt. of extracted oil” is the weight of the oil after extraction and drying in the vacuum evaporator; “wt. of waste fish” is the mass of the waste fish. The physico-chemical properties of the oil, such as the acid value, iodine number, and saponification index, were determined by the ASTM D 664, D 5554, and D 5558 methods, respectively, and are reported in Table 1.

2.3. Fatty acid composition

For the fatty acid composition, a BF3-method was used after derivatization in fatty acid methyl esters (FAMEs) [76]. FAMEs analysis was performed by using a GC–MS, Thermo-Fischer gas chromatography

equipment. A capillary column, Trace-GOLD TG-POLAR GC Columns 0.25 µm × 0.25 mm× 60 m, was used. Helium was the carrier gas at 1.2 ml/min. In detail: detector and inlet temperature: 250 ◦C; initial temperature 150 ◦C up to 190 ◦C, 15 ◦C/min, and 5 min at 190 ◦C; finally, the temperature was raised to 230 ◦C, 4 ◦C/min, and 10 min at 230 ◦C. For peak identification, a certified reference FAME mixture (C14-C24) was used to compare retention times.

2.4. Synthesis of amino hyper cross-linked resin

Amino-functionalized hypercross-linked resins based on divinylbenzene/vinyl benzyl chloride were synthesized as reported by Castaldo et al. [77]. The monomers (divinylbenzene/vinyl benzyl chloride, 2:98 molar ratio) were mixed under nitrogen, and then bulk polymerization was performed with 2,2'-azobis(2-methyl-propionitrile) for 6 h at 80 ◦C. After that, the precursor resin was purified and subjected to the Friedel-Crafts reaction using a catalyst (ferric chloride, $FeCl_3$) and a swelling agent (1,2-dichloroethane) to obtain the hypercross-linked resin (HCLR). The amino-modified hypercross-linked resin was obtained starting from the as-obtained neat HCLR through a nitration-reduction process. HCLR was added to a mixture of nitric acid/sulfuric acid/water ($HNO_3/H_2SO_4/H_2O$, 75/20/5 vol%) that was kept in an ice bath under N_2 flux. The reaction mixture was agitated for 1 h, and then the mixture was poured slowly into a sodium hydroxide solution (NaOH, 10 M). The product was separated by filtration, washed with distilled water until pH = 7, and dried in a vacuum oven at 80 ◦C to obtain HCLR-NO_2. HCLR-NO_2 underwent a reduction process with stannous chloride ($SnCl_2$) in a 1/1 vol/vol hydrochloric acid/ethanol solution. The reaction mixture was stirred at 60 ◦C under N_2 for 2 h. The resulting resin was washed with a diluted H_2SO_4 solution, neutralized with distilled H_2O, and dried under vacuum at 80 ◦C to obtain HCLR-NH_2.

2.5. Preparation of magnetic HCLR-NH_2 support and Fe_3O_4 NPs

To prepare magnetic amino hypercross-linked resin (M-HCLR-NH_2, Fig. 2) [78], 500 g of amino resin was dispersed in 20 ml of water for 24 h in a 50 ml round-bottom flask. Then, 79.5 mg of ferrous chloride tetrahydrate ($FeCl_2 \bullet 4\ H_2O$) and 216.3 mg of ferric chloride hexahy- drate ($FeCl_3 \bullet 6\ H_2O$) were added, and the solution was evacuated at 25 ◦C for 3 days. Finally, the vacuum was removed, the suspension was centrifuged, and the product was redispersed in water (10 ml). The mixture was heated to 80 ◦C with 25% aqueous ammonia (74 µl) for 30 min. After 30 min, the magnetic resin (M-HCLR-NH_2) was washed several times in water. The synthesis of Fe_3O_4 NPs alone was carried out under the same experimental conditions but in the absence of the amino-modified hypercrosslinked resin. Amino-functionalized Fe_3O_4 NPs were then obtained by a nitrification-reduction process, following the same procedure as previously described for HCLR-NH_2 surface modification.

2.6. Enzyme immobilization

Candida rugosa lipase was immobilized onto amino-terminated magnetic resin (M-HCLR-NH_2 support) by ion exchange, interfacial activation, and covalent immobilization. In particular, the covalent bond between the carboxyl groups of lipase and the M-HCLR-NH_2 sup- port was mediated by 1-ethyl-3-(3-dimethylaminopropyl) carbodiimide (EDC) [79,80]. EDC was used for enzyme immobilization because it is water-soluble, eco-friendly, and noncytotoxic [81,82]. Furthermore, it is called a zero-length cross-linking agent because it activates carboxyl groups and mediates the linkage with superficial primary amino groups without the use of any spacer molecules, which can generate random bonds, blocking enzyme active sites [83]. Briefly, a solution containing 2.5 g/l of enzyme and 0.4 g/l of EDC in20 ml of a potassium sodium-phosphate buffer (pH 7, 0.1 M) was incubated at 4 ◦C at 200 rpm for 30 min. Subsequently, a 5 mg/ml suspension of M-HCLR-NH_2 support

in 20 ml of potassium sodium phosphate buffer was added to the EDC-lipase solution (0.5 enzyme/ support wt. ratio) and incubated at 4 ◦C and 200 rpm for various times. After the coupling time, the immobilized lipase (M-HCLR-NH2 @CRL) was removed by an external magnetic field and washed several times with phosphate buffer to remove the excess unbound lipase and, finally, tested for the lipase assay. Candida rugosa lipase was also immobilized onto Fe3O4 NPs under the same experimental conditions (Fe3O4 @CRL). Briefly, a solution containing 2.5 g/l of enzyme and 0.4 g/l of EDC in 20 ml of a potassium sodium-phosphate buffer (pH 7, 0.1 M) was incubated at 4 ◦C at 200 rpm for 30 min. Subsequently, a 5 mg/ml suspension of amino-functionalized Fe3O4 in 20 ml of potassium sodium-phosphate buffer (pH 7, 0.1 M) was added to the EDC-lipase solution and incubated at 4 ◦C and 200 rpm for various times. After the coupling time, Fe3O4 @CRL was removed by an external magnetic field and washed several times.

2.7. Determination of immobilization efficiency, immobilization yield, and lipase activity

Bradford's method was used to evaluate the amount of enzyme loaded on the support using bovine serum albumin (BSA) as a standard [84]. The data used were averages of two different tests. In particular, the amount of lipase was determined by the difference between the enzyme unbounded in the supernatant and the initial enzyme amount. Therefore, the immobilization efficiency was expressed as (Eq 2).

$$Immobilization \quad efficiency = \frac{C_O - C_s}{C_o} \qquad (2)$$

where Co and Cs are the initial concentration and the final unbound concentration in the supernatant in the immobilization reaction, respectively.

Immobilized yield is defined as the ratio between the hydrolytic activity immobilized on the support surface at equilibrium (initial activity – residual activity) and initial activity [69]. The lipase activities of soluble and immobilized lipase were determined by the hydrolysis method [39,85]. Briefly, soluble and immobilized lipase were reacted in 5 ml of olive oil (highly refined-low acidity, CAS 8001–25–0) emulsion and 6 ml of 0.1 M phosphate buffer solution at pH 7. The soluble/immobilized lipase was incubated for 30 min at 37 ◦C under shaking. Subsequently, the amount of fatty acid liberated was obtained by titration using a 0.1 M potassium hydroxide solution using a phenolphthalein indicator. Moreover, the hydrolysis reaction for soluble/immobilized lipase was also evaluated at different temperatures for 30 min. One unit (U) of catalytic activity was defined as the amount of enzyme able to hydrolyse 1 µmol/min of fatty acid. Moreover, activity recovery % is defined as the ratio of the M-HCLR-NH2 @CRL activity to the activity of soluble lipase. Measurements were performed in triplicate, and the mean values, as well as standard deviations and coefficients of variation, were reported.

2.8. Transesterification reaction

Transesterification, kinetically controlled [28,29], is the main reaction mechanism. However, the possibility that esterification reactions, thermodynamically controlled [30,31], may also occur, given the pres- ence of free FFA and, to some extent, hydrolysis, cannot be ignored. The reactions were conducted in a 50 ml round-bottom flask under mechanical stirring at 40 ◦C and at different times. The reaction mixture consisted of waste fish oil (10 g), oleyl alcohol with a molar ratio (1:3 oil/alcohol), bionanocatalyst (10–25% wt./wt. of oil), and 20 ml of solvent (n-hexane). The solvent choice is extremely important. Indeed, performing the reaction in a solvent can have several advantages [86]: improved solubility of hydrophobic substrates, favoured thermodynamic equilibrium during hydrolysis, and favoured enzyme thermostability. The degree of polarity

of the solvent is a key element. It is necessary to choose solvents with an appropriate partition coefficient (log P) to avoid disturbing the minimum quantity of water in the proximity of the enzyme, which is necessary for enzymatic function [87]. Solvents that are too hydrophobic (logP> 4) could have negative effects on the solubility of the reagents. Hexane can be considered a good compromise [88]; it allows a favourable viscosity for the reaction mixture, improving mass transfer vs. enzyme active sites [89]. After the transesterification time, the M-HCLR-NH2 @CRL was recovered by an external magnetic field. A rotary vacuum evaporator was used to remove the solvent at 70 ◦C. To further purify the esters from glycerol, ethanol was added to the mixture. Glycerol and alcohol residues, which are soluble in ethanol were finally removed using a separator funnel. Finally, the esters were additionally purified using a rotary vacuum evaporator to remove the residual ethanol. As the last step, the sample was analysed by GC–MS. Furthermore, the effect of molar ratio, reaction temperature, and reusability was also investigated.

Transesterification reactions were also performed with free Candida rugosa lipase and Candida rugosa lipase immobilized on Fe3O4 NPs (Fe3O4 @CRL) under the same experimental conditions. Free lipase residue from the previous purification procedure of the esters was washed with distilled water.

2.9. GC–MS product analysis

The reaction mixture was analysed using a Thermo-Fischer gas chromatograph equipped with Trace-GOLD TG-POLAR GC Columns (60 m × 250 µm; film thickness 0.25 µm). A 1 µl aliquot of sample was injected into a split mode GC. The initial temperature was 150 ◦C, maintained for 2 min, then the temperature was increased to 250 ◦C at 20 ◦C/min, and, finally, 14 min at 250 ◦C. The detector and inlet temperatures were 250 ◦C and 260 ◦C, respectively. Helium was used as the carrier gas, and the flow rate was 25 ml/min. Methyl heptadecanoate was used as an internal standard for product quantification. Methyl heptadecanoate was used as an internal standard because it is not pre- sent in the oil considered and does not overestimate the final product. In particular, a sample of 1 µl was obtained by mixing 150 µl of methyl heptadecanoate solution (5 mg/ml) with 200 µl of product and 1.15 ml of hexane.

The target component concentration was evaluated from the relationship between the peak area ratio and the concentration ratio of the target component and the internal standard. In particular, the concentrations of esters were calculated using the following equation [90] (Eq. Based on the ester concentrations, the moles of the ester were calculated, and the percentage yield (Eq. 4) was determined.

$$C_E(mg \Big/ ml) = \left(\frac{A_E}{A_{IS}}\right) \times \frac{C_{IS} \quad D_{R,IS}}{D_{R,E}} \tag{3}$$

$$yield(\%) = \frac{mmol \quad of \quad ester}{3 \times mmol \quad waste \quad fish \quad oil} \times 100\% \tag{4}$$

where CE and CIS are the amounts of E in esters or inside the internal standard, respectively, AE = peak area of component E, AIS = peak area of the internal standard, and DR,IS, and DR,E are the detector response factors for the internal standard and component E, respectively. The physicochemical properties of the esters, such as the acid value, specific gravity, pour point, and iodine number, were determined by the ASTM D 664, D 4052, and D 5554 methods, respectively. All measurements were performed in triplicate.

2.10. Catalyst characterization

Nanocatalyst samples were monitored under SEM (scanning electron microscopy) (TESCAN-VEGA LMH; 230 V) coupled with an EDS probe. For thermogravimetric studies, TGA 2, METTLER TOLEDO, was used under an airflow at 10 ◦C/min. FT-IR spectra were obtained by Nicolet iS50 FT-IR. X-ray diffraction measurements were also performed by a Bruker D2 X-ray diffractometer using CuKα radiation.

3. Results and discussion

3.1. Fatty acid composition and physicochemical characteristics

The yield of oil extracted from waste fish was approximately 30% ± 2.0. The fatty acid composition and the GC profile of the extracted oil are depicted in Table 1 and Fig. 3. The oil sample is made up of saturated acids (SFA) 24.85% ± 2.1; monounsaturated acids (MUFA) 47.30% ± 1.8; and, polyunsaturated fatty acids (PUFA) 27.84% ± 2.2. In particular, the oil contained C16:0 (16.64%) as the most abundant saturated fatty acid, followed by C14:0 (4.10%) and C18:0 (3.64%). The total unsaturated fatty acids (MUFA+PUFA) of the waste fish oil was 75.15% ± 1.4; 1.49% and 8.06% were due to the presence of omega-3, C20:5n3, and C22:6n3, respectively. The physicochemical characteristics of the extracted oil from waste fish are shown in Table 2, including moisture content, free fatty acid amount, acid value, iodine value, and saponification index.

3.2. Nanohybrid Characterization

Scanning electron microscopy (SEM) images of HCLR-NH2 and M- HCLR-NH2 are depicted in Fig. 4. The SEM image of HCLR-NH2, Fig. 4a, shows surface dense and compact structures. After iron precipitation, in HCLR-NH2, the SEM images of M-HCLR-NH2 show no large aggregates of iron oxides on the surface and between particles (Fig. 4b). More detailed SEM-EDX studies of the magnetic support show that Fe3O4 nanoparticles are distributed over the HCLR-NH2, Fig. 4c, and maps of C, Fe, and O at the bottom of Fig. 4.

3.3. XRD studies

In the XRD pattern of Fe3O4 (Fig. 5), the typical peaks of magnetite [91] can be observed. The XRD spectrum of HCLR-NH2 (Fig. 5) shows a wide, weak band, indicating an almost amorphous structure. Finally, the diffraction pattern of M-HCLR-NH2 is also reported in Fig. 5, showing characteristic peaks similar to those of Fe3O4 at 34.68◦, 42.71◦, 56.69◦, and 62.19◦, corresponding to the (311), (400), (422), (511), and (440) Fe3O4 Bragg reflections [39,92,93], indicating the formation of magnetite NPs, likely in the resin mesopores. In particular, an average crystallite size of approximately 13 nm was calculated from the line broadening of the strongest diffraction peak in the (311) plane using the Scherrer equation [92,93].

3.4. Thermogravimetric analysis (TG-DTG)

In Fig. 6, the thermogravimetric profiles of the amino hyper cross- linked resin (HCLR-NH2), the magnetic amino hyper cross-linked resin (M-HCLR-NH2), magnetic amino hyper cross-linked resin after lipase immobilization (M-HCLR-NH2 @CRL), and Candida rugosa lipase (Sigma Aldrich) are shown. In particular, the TG curve of HCLR-NH2 exhibits a main weight loss in the range 230–590 ◦C, in which the HCLR-NH2 support

is completely degraded. M-HCLR-NH2 presents a residual weight of approximately 12%. This residual weight, which is due to the content of magnetite in the resin, accelerates the degradation of the polymeric phase in the nanocomposites. The TG profile of M-HCLR-NH2 @CRL shows successful lipase immobilization.

3.5. FT-IR analysis

The FT-IR spectra of the amino hyper cross-linked support (HCLR- NH2), magnetic amino hyper cross-linked support (M-HCLR-NH2), and immobilized enzyme (M-HCLR-NH2 @CRL) are depicted in Fig. 7. The HClR-NH2 spectrum shows the –CH2 bending vibration at 1435 cm-1 and the intense band at 1645 cm-1 due to the –NH2 bending vibrations. The band at 3329 cm-1 can be assigned to N-H stretching [94,95]. After the precipitation of iron in HCLR-NH2, the spectrum of M-HCLR-NH2 shows a shift of the band from 570 cm-1 to 560 cm-1 due to the bending vibration of Fe-O [93,96]. The spectrum of free lipase is depicted in Fig. 7 insert, and the major protein vibrational bands due to the peptide group vibrations occur in the range 1200–1900 cm-1. The amide I band, attributable to the C–O stretching vibration, is visible at 1700 cm-1; the amide II band is visible at 1560 cm-1 due to N-H bending, while the C-N stretching vibration at 1384 cm-1 corresponds to the amine III band; moreover, in the 900–1200 cm-1 range, the vibrational bands due to the sugar chain of the lipase can be seen [38,39,97]. After immobilization (M-HCLR-NH2 @CRL), EDC-mediated favouring carboxyl group linkage with superficial amino groups without introducing any spacer molecules (zero-length crosslinking agent), the FT-IR spectrum showed that the lipase amide I band shifted at 1651 cm-1; furthermore, the immobilized CRL displayed broadened bands and shifted peaks, thereby validating a conformational change of the enzyme due to chemical linkages [98]. In Fig. 8, a schematic illustration of the EDC-mediated reaction is shown. The reaction occurs in two steps (see Fig. 8): first, the carboxyl groups of the enzyme are activated by adding EDC, and an active intermediate product is formed, followed by enzyme addition through a peptide bond between the carboxyl groups of the lipase and the superficial amino group of the support surface. The IR spectrum modifications for M-HCLR-NH2 @CRL at approximately 1600 cm-1 can also suggest physical interactions occurring due to ion exchange.

3.6. Immobilization efficiency, immobilization yield, and activity recovery

To ascertain the proper incubation time of lipase for the immobili- zation process, different immobilization times from 1 h to 6 h were evaluated in lipase solution (2.5 g/L) and with 0.1 g of magnetic sup- port. As indicated in Fig. 9a, the immobilization efficiency on the magnetic support, due to residual active amino groups still available on the surface of the magnetic support for immobilization, gradually increased as the incubation time increased in the investigated range. The lipase activity recovery increases up to 94% at 5 h. This is probably due not only to improved conformation flexibility in the interaction with the substrate molecules but also to the opening of the lipase lid when it interacts with the resin hydrophobicity. An immobilization efficiency of 95%, immobilized yield of 90%, and a protein loading of 475 mg/g of support at equilibrium were achieved after 5 h [69,99]. On the other hand, after this time, the activity recovery decreases, as previously observed in several studies [100–102]. In the absence of EDC-mediated bonds, the low immobilization efficiency (approximately 16%) may be due to physical interactions, such as interfacial activation and ion ex- change between the resin and the enzyme. From the above results, it is reasonable to suggest that covalent EDC-mediated immobilization oc- curs and that the proper incubation time for 2.5 g/L lipase solution is 5 h.

Temperature is one of the main parameters affecting enzymatic activity. The relative activity [99] for different temperatures between 20 and 60 ◦C was determined, and the results are given in Fig. 9b. The optimum temperature for the soluble enzyme was 35 ◦C, while the immobilized enzyme showed the highest activity at

45 ◦C. Moreover, in the temperature range of 20–60 ◦C, the immobilized enzyme on the magnetic resin results in less sensitivity to the temperature change, probably due to support inducing stability.

3.7. Ester synthesis: effect of operating variables

The effect of reaction time on the transesterification of the waste oil is shown in Fig. 10a. In particular, the conversion of the waste oil with oleyl alcohol was investigated at different reaction times under the same process conditions. The conversion was found to be relatively low over the first 8 h of reaction (up to 62%) but increased to 85% after 12 h. A further reaction time increase, up to 24 h, led only to an additional 2% substrate conversion. Consequently, all further catalytic tests for the transesterification of waste oil mediated by immobilized enzyme were performed for a period of 12 h. The relatively low degree of substrate conversion at a longer reaction time is likely due to enzyme specificity [103].

The effect of reaction temperature was examined at various temperatures, ranging from 40 ◦C to 60 ◦C, as shown in Fig. 10b. The highest ester yield was achieved at 45 ◦C (87%). The ester yield slowly decreases at higher reaction temperatures, which might account for the denaturation of the lipase as well as an alteration in the 3-D structure of lipase [104]. The temperature profile demonstrated that the optimum temperature for wax ester synthesis was 45 ◦C.

The effect of immobilized enzyme concentration during wax ester synthesis was also investigated (see Fig. 10c). The amount of lipase plays a crucial role in any biocatalytic process, and its influence on the reaction was assessed to determine a suitable enzyme amount for achieving good yields. The ester conversion increases rapidly as the immobilized lipase amount increases from 10% and 15% wt./wt. (mg of enzyme per mg of oil). At 15% wt./wt. of lipase, a maximum conversion of 91% after 12 h was achieved. In Fig. 10d, the effect of the oil:alcohol molar ratio on the transesterification reaction is shown. The optimal oil:alcohol molar ratio was 1:4 with a maximum conversion of ~94%. Increasing the molar ratio of oil to alcohol beyond 1:4 decreases the trans- esterification activity. This observation may reflect the fact that alcohol can deviate the essential water layer from the enzyme [105]. At the same time, excess alcohol hinders the interaction of lipase with the acid sur- face [106]. From the above results, it is reasonable to suggest that the proper reaction condition was 15% of the immobilized enzyme with 1:4 oil:alcohol molar ratio for 12 h at 45 ◦C.

In Fig. 11, a comparison of the ester synthesis of M-HCLR-NH2 @CRL, Fe3O4 @CRL, and free lipase (CRL) is shown under the optimal conditions. In particular, M-HCLR-NH2 @CRL showed higher activity, with a yield of approximately 94%, than Fe3O4 @CRL and free lipase (CRL), with yields of 80% and 65%, respectively. This is due to the ability of the HCLR-NH2 support to allow, during the immobilization process, high loading of the highly active enzyme stabilized on the matrix hypercrosslinked network structure preventing extensive structural changes during the transesterification, and probably the alcohol preconcentration in HCLRs, favouring the reaction and protecting the external surface-anchored enzyme, which is sensitive to alcohol excesses. On the other hand, EDC, directly reacting with the functionalized resin, allows a zero-length strong covalent conjugation between the enzyme and the resin [107], which led to a dramatic increase in catalytic activity due to the direct interaction of the lid of the enzyme with the resin hydrophobic structure by interfacial activation phenomena [98].

The main purpose of using immobilized lipase is to retain the activity during subsequent cycles, which is essential for practical applications of the process. To investigate the reusability, immobilized lipase was removed from the reaction mixture with an external magnetic field and washed with n-hexane to remove any substrate or product. As indicated in Fig. 12, the conversions to wax esters remain constant at 94% after the first five uses. Furthermore, after five uses, the catalyst maintains a conversion of 90%, showing excellent reusability. The results of the catalyst reusability also suggest that enzyme loss, which cannot be completely neglected, is not significant. This result confirmed that the CRL immobilized on M-HCLR-NH2 allowed not only

excellent activity but also satisfactory reusability in several reaction cycles. The retention of enzymatic activity and fine reproducibility can be attributed to the mild synthesis conditions and the robust immobilization ability of the magnetic resin matrix, which does not affect active sites and subunits. The choice to work in a solvent, in particular hexane, favours solubility for hydrophobic substrates; low viscosity for improved mass transfer; right polarity to avoid disturbing the minimum amount of water in the proximity of the enzyme, which is necessary for enzymatic function; thermodynamic equilibrium during hydrolysis; and enzyme thermostability, which cannot be ignored. On the other hand, due to the affinity of the support with water, a role in favouring its correct availability cannot be neglected.

The performance of CRL immobilized on M-HCLR-NH2 in the synthesis of wax ester was compared with the literature results [108–114], as shown in Table 3. The prepared biocatalyst showed activity compa- rable, if not higher, to other biocatalysts and good reusability. These results confirm the promising application of the prepared biocatalyst in wax ester synthesis.

3.8. Esters characterization

The wax esters produced via transesterification of oleyl alcohol with waste fish oils and using immobilized lipase were further characterized and compared with the waste fish oil. In particular, the ester was characterized by the acid value, the saponification value, the specific gravity, and the iodine number (Table 4). Generally, both waste fish oil and esters were orange in colour, but the orange colour of the ester was very light (see Fig. 13). The specific gravity and saponification value of the ester were much lower than those of the waste oil, likely due to the lower molecular weight of the esters. On the other hand, the iodine number of the esters was higher than that of the waste fish oil due to the introduction of the additional double bond of the oleyl alcohol. Finally, the lower acid value is a further advantage, as it does not impair oxidative stability and prevents rancidity [115].

4. Conclusion

A novel magnetic amino hypercross-linked resin was prepared and used as a carrier for the immobilization of inexpensive CRL by ion ex- change, interfacial activation, and covalent bonds mediated by EDC. The characterization highlights the uniform distribution of the magnetic nanoparticles in the HCLR structure, allowing easy separation of the catalyst for subsequent cycles.

The results of the experiments allow us to highlight the successful choice of HCLR support for immobilization, stabilization, and preser- vation of the catalyst. By exploiting the surface functionalization of the resin, it was possible to easily anchor the biocatalyst with high yields. HCLRs not only act as a catalyst immobilizing structure but also, more advantageously, as a preconcentrating structure for alcohol, incorporating one of the reagent's nearby enzyme active sites. This results in favouring of the reaction and protection of the external surface- anchored enzyme, which is sensitive to excess alcohol.

In conclusion, due to the advantages of a large surface area, special surface structure, and desirable functionalities, M-HCLR-NH2 @CRL allows high catalytic performance with increased thermal stability and reusability in ester synthesis.

The use of an enzymatic catalyst with different functionalities to respond to different process needs has been demonstrated in the production of a high-added value wax, the properties of which have also been evaluated.

Declaration of Competing Interest

The authors declare that they have no known competing financial interests or personal relationships that could have appeared to influence the work reported in this paper.

Data Availability

Data will be made available on request.

References

[1] N.R. Khan, S.V. Jadhav, V.K. Rathod, Lipase catalysed synthesis of cetyl oleate using ultrasound: Optimisation and kinetic studies, Ultrason. Sonochem. 27 (2015) 522–529, https://doi.org/10.1016/j.ultsonch.2015.03.017.
[2] K.N.P. Rani, T.S.V.R. Neeharika, T.P. Kumar, B. Satyavathi, C. Sailu, R.B.N. Prasad, Kinetics of enzymatic esterification of oleic acid and decanol for wax ester and evaluation of its physico-chemical properties, J. Taiwan Inst. Chem. Eng. 55 (2015) 12–16, https://doi.org/10.1016/j.jtice.2015.04.011.
[3] E.H.M. Size, Share Trends Analysis Report by Product. By Application, by Region, and Segment Forecasts (2020) 2027.
[4] E.C.G. Aguieiras, A. Papadaki, A. Mallouchos, I. Mandala, H. Sousa, D.M.G. Freire, A.A. Koutinas, Enzymatic synthesis of bio-based wax esters from palm and soybean fatty acids using crude lipases produced on agricultural residues, Ind. Crops Prod. 139 (2019), 111499, https://doi.org/10.1016/j. indcrop.2019.111499.
[5] Anon, 2016. The Global Wax Industry Is Bound to Experience Future Shortages, Sees Kline. (accessed 30 November 2022). 〈https://www.prnewswire.com/new s-releases/the-global-wax-industry-is-bound-to-experience-future-shortages-sees-kline-300211445.html〉.
[6] F. Domergue, M. Miklaszewska, The production of wax esters in transgenic plants: towards a sustainable source of bio-lubricants, J. Exp. Bot. 73 (2022) 2817–2834, https://doi.org/10.1093/jxb/erac046A.
[7] A.E.V. Petersson, L.M. Gustafsson, M. Nordblad, P. Bo¨rjesson, B. Mattiasson,
P. Adlercreutz, Wax esters produced by solvent-free energy-efficient enzymatic synthesis and their applicability as wood coatings, Green. Chem. 7 (2005) 837–843, https://doi.org/10.1039/B510815B.
[8] K.N. Prasanna Rani, T.S.V.R. Neeharika, T. Prathap Kumar, B. Satyavathi, Ch Sailu, R.B.N. Prasad, Kinetics of enzymatic esterification of oleic acid and decanol for wax ester and evaluation of its physico-chemical properties, J. Taiwan Inst. Chem. Eng. 55 (2015) 12–16, https://doi.org/10.1016/j. jtice.2015.04.011.
[9] N.R. Khan, V.K. Rathod, Enzyme catalyzed synthesis of cosmetic esters and its intensification: a review, Process Biochem 50 (2015) 1793–1806, https://doi. org/10.1016/j.procbio.2015.07.014.
[10] M.D. Alves, E´.C. Cren, A.A. Mendes, Kinetic, thermodynamic, optimization and reusability studies for the enzymatic synthesis of a saturated wax ester, J. Mol. Catal., B Enzym 133 (2016) S377–S387, https://doi.org/10.1016/j. molcatb.2017.02.011
[11] P. Ungcharoenwiwat, A. H-Kittikun, Enzymatic synthesis of coconut oil based wax esters by immobilized lipase EQ3 and commercial lipozyme RMIM, Electron.
J. Biotechnol. 47 (2020) 10–16, https://doi.org/10.1016/j.ejbt.2020.06.005.
[12] P. Ungcharoenwiwat, A.H. Kittikun, Purification and characterization of lipase from Burkholderia sp. EQ3 isolated from wastewater from a canned fish factory and its application for the synthesis of wax esters, J. Mol. Catal. B Enzym 115 (2015) 96–104, https://doi.org/10.1016/j.molcatb.2015.02.005.
[13] Y.-H.V. Soong, L. Zhao, N. Liu, P. Yu, C. Lopez, A. Olson, H.-W. Wong, Z. Shao, D. Xie, Microbial synthesis of wax esters, Metab. Eng. 67 (2021) 428–442, https://doi.org/10.1016/j.ymben.2021.08.002.

[14] C.H. Kuo, H.H. Chen, J.H. Chen, Y.C. Liu, C.J. Shieh, High yield of wax ester synthesized from cetyl alcohol and octanoic acid by Lipozyme RMIM and Novozym 435, Int. J. Mol. Sci. 13 (2012) 11694–11704, https://doi.org/ 10.3390/ijms130911694.
[15] A.E. Ghaly, V.V. Ramakrishnan, M.S. Brooks, S.M. Budge, D. Dave, Fish processing wastes as a potential source of proteins, amino acids and oils, a critical review, J. Microb. Biochem. Technol. 5 (2013) 107–129, https://doi.org/ 10.4172/1948-5948.1000110.
[16] D. Dave, V.V. Ramakrishnan, S. Trenholm, H. Manuel, J. Pohling, W. Murph, Marine oils as potential feedstock for biodiesel production: physicochemical characterization, J. Bioprocess Biotech. 4 (2014) 1–12, https://doi.org/10.4172/2155-9821.1000168.
[17] K. Kara, F. Ouanji, El M.Lotfi, M. ElMahi, M. Kacimi, M. Ziyad, Biodiesel production from waste fish oil with high free fatty acid content from Moroccan fish-processing industries, Egypt. J. Pet. 27 (2018) 249–255, https://doi.org/ 10.1016/j.ejpe.2017.07.010.
[18] S. Espootin, M. Sameti, S. Zaker, Biodiesel from fish waste oil: synthesis via supercritical methanol and thermodynamic optimization, Clean. Energy 5 (2021) 187–195, https://doi.org/10.1093/ce/zkab003.
[19] T.G. Kudre, N. Bhaskar, P.Z. Sakhare, Optimization and characterization of biodiesel production from rohu (Labeo rohita) processing waste, Renew. Energy 113 (2017) 1408–1418, https://doi.org/10.1016/j.renene.2017.06.101.
[20] B. Angulo, J.M. Fraile, L. Gil, C.I. Herrerías, Bio-lubricants production from fish oil residue by transesterification with trimethylolpropane, J. Clean. Prod. 202 (2018) 81–87, https://doi.org/10.1016/j.jclepro.2018.07.260.
[21] A.S. Al Hatrooshi, V.C. Eze, A.P. Harvey, Production of biodiesel from waste shark liver oil for biofuel applications, Renew. Energ. 145 (2020) 99–105, https://doi. org/10.1016/j.renene.2019.06.002.
[22] A.B. Fadhil, A.I. Ahmed, Production of mixed methyl/ethyl esters from waste fish oil through transesterification with mixed methanol/ethanol system, Chem. Eng. Commun. 205 (2018) 1157–1166, https://doi.org/10.1080/00986445.2018.1434514.
[23] P. Ungcharoenwiwat, A. H-Kittikun, Purification and characterization of lipase from Burkholderia sp. EQ3 isolated from wastewater from a canned fish factory and its application for the synthesis of wax esters, J. Mol. Catal. B Enzym 115 (2015) 96–104, https://doi.org/10.1016/j.molcatb.2015.02.005.
[24] P. Ungcharoenwiwat, A. H-Kittikun, Synthesis of wax esters from crude fish fat by lipase of burkholderia sp. EQ3 and commercial lipases, J. Am. Oil Chem. Soc. 90 (2013) 359–367, https://doi.org/10.1007/s11746-012-2183-y.
[25] R. Abuine, A.U. Rathnayake, H.-G. Byun, Biological activity of peptides purified from fish skin hydrolysates, Fish. Aquat. Sci. 22 (2019) 10, https://doi.org/ 10.1186/s41240-019-0125-4.
[26] A.P. Harnedy, R.J. FitzGerald, Bioactive peptides from marine processing waste and shellfish: a review, JFF 4 (2012) 6–24, https://doi.org/10.1016/j. jff.2011.09.001.
[27] S.B. Gaikwad, P.R. More, S.K. Sonawane, S.S. Arya, Antioxidant and anti- hypertensive bioactive peptides from Indian mackerel fish waste, Int. J. Pept. Res. Ther. 27 (2021) 2671–2684, https://doi.org/10.1007/s10989-021-10282-0.
[28] V. Kasche, B. Galunsky, G. Michaelis, Binding of organic solvent molecules influences the P1'-P2' stereo and sequence specificity of a-chymotrypsin in kinetically controlled peptide synthesis, Biotechnol. Lett. 13 (1991) 75–80, https://doi.org/10.1007/BF01030454.
[29] S.R. Marsden, L. Mestrom, D.G.G. McMillan, U. Hanefeld, Thermodynamically and kinetically controlled reactions in biocatalysis – from concepts to perspectives, ChemCatChem 12 (2020) 426–443, https://doi.org/10.1002/ cctc.201901589.
[30] V. Kasche, U. Haufler, L. Riechmann, Equilibrium and kinetically controlled synthesis with enzymes: semisynthesis of penicillins and peptides, Meth. Enzymol. 136 (1987) 280–292.
[31] V. Kasche, Mechanism and yields in enzyme catalysed equilibrium and kinetically controlled synthesis of β-lactam antibiotics, peptides and other condensation products (1986), Enzym. Microb. Technol. 8 (1986) 4–16.
[32] B. Thangaraj, P.R. Solomon, B. Muniyandi, S. Ranganathan, L. Lin, Catalysis in biodiesel production—a review, Clean. Energy 3 (2019) 2–23, https://doi.org/ 10.1093/ce/zky020.

[33] R. Cui, S. Ma, B. Yang, S. Li, T. Pei, J. Li, J. Wang, S. Sun, C. Mi, Simultaneous removal of NOx and 384 SO2 with H2O2 over silica sulfuric acid catalyst synthesized from fly ash, Waste Manag. 109 (2020) 65–74, https://doi.org/ 10.1016/j.wasman.2020.04.049.
[34] R. Bandikari, J. Qian, R. Baskaran, Z. Liu, G. Wu, Bio-affinity mediated immobilization of lipase onto magnetic cellulose nanospheres for high yield biodiesel in one time addition of methanol, Bioresour. Technol. 249 (2018) 354–360, https://doi.org/10.1016/j.biortech.2017.09.156.
[35] F. Benamia, S. Benouis, A. Belafriekh, N. Semache, N. Rebbani, Z. Djeghaba, Efficient Candida rugosa lipase immobilization on Maghnite clay and application for the production of (1R)-(2)-Menthyl acetate, Chem. Pap. 71 (2016) 785–793, https://doi.org/10.1007/s11696-016-0080-9.
[36] S. Arana-Pen˜a, D. Carballares, A´. Berenguer-Murcia, A.R. Alc´antara, R.
C. Rodrigues, R. Fernandez-Lafuente, One pot use of combilipases for full modification of oils and fats: multifunctional and heterogeneous substrates, Catalysts 10 (2020) 605.
[37] M. Sarno, M. Iuliano, Active biocatalyst for biodiesel production from spent coffee ground, Bioresour. Technol. 266 (2018) 431–438, https://doi.org/10.1016/j. biortech.2018.06.108.
[38] M. Iuliano, M. Sarno, S. De Pasquale, E. Ponticorvo, Candida rugosa lipase for the biodiesel production from renewable sources, Renew. Energy 162 (2020)
124–133, https://doi.org/10.1016/j.renene.2020.08.019.
[39] M. Sarno, M. Iuliano, G_Fe3O4/Ag supporting Candida rugosa lipase for the “green” synthesis of pomegranate seed oil derived liquid wax esters, Appl. Surf. Sci. 510 (2020), 145481, https://doi.org/10.1016/j.apsusc.2020.145481.
[40] J.M. Bolivar, J.M. Woodley, R. Fernandez-Lafuente, Is enzyme immobilization a mature discipline? Some critical considerations to capitalize on the benefits of immobilization, Chem. Soc. Rev. 51 (2022) 6251–6290, https://doi.org/ 10.1039/D2CS00083K.
[41] R.C. Rodrigues, A´. Berenguer-Murcia, D. Carballares, R. Morellon-Sterling,
R. Fernandez-Lafuente, Stabilization of enzymes via immobilization: multipoint covalent attachment and other stabilization strategies, Biotechnol. Adv. 52 (2021), 107821, https://doi.org/10.1016/j.biotechadv.2021.107821.
[42] R.C. Rodrigues, J.J. Virgen-Ortíz, J.C.S. dos Santos, A´. Berenguer-Murcia, A. R. Alcantara, O. Barbosa, C. Ortiz, R. Fernandez-Lafuente, Immobilization of lipases on hydrophobic supports: immobilization mechanism, advantages, problems, and solutions, Biotechnol. Adv. 37 (2019) 746–770.
[43] C. Bernal, K. Rodríguez, R. Martínez, Integrating enzyme immobilization and protein engineering: an alternative path for the development of novel and improved industrial biocatalysts, Biotechnol. Adv. 36 (2018) 1470–1480, https:// doi.org/10.1016/j.biotechadv.2018.06.002.
[44] A. De Simone, M. Naldi, M. Bartolini, L. Davani, V. Andrisano, Immobilized enzyme reactors: an overview of applications in drug discovery from 2008 to 2018, Chromatographia 82 (2019) 425–441, https://doi.org/10.1007/s10337-018-3663-5.
[45] A.A. Homaei, R. Sariri, F. Vianello, R. Stevanato, Enzyme immobilization: an update, J. Chem. Biol. 6 (2013) 185–205, https://doi.org/10.1007/s12154-013-0102-9.
[46] M. Sarno, M. Iuliano, M. Iuliano, P. Ciambelli, High activity and selectivity immobilized lipase on Fe3O4 nanoparticles for banana flavor synthesis, Process Biochem 56 (2017) 98–108.
[47] U. Hanefeld, L. Gardossi, E. Magner, Understanding enzyme immobilisation, Chem. Soc. Rev. 38 (2009) 453–468.
[48] V.R. Murty, J. Bhat, P.K.A. Muniswaran, Hydrolysis of oils by using immobilized lipase enzyme: a review, Biotechnol. Bioprocess Eng. 7 (2002) 57–66.
[49] H. Gao, L. Ding, H. Bai, A. Liu, S. Li, L. Li, Pitch-based hyper-cross-linked polymers with high performance for gas adsorption, J. Mater. Chem. A 4 (2016) 16490–16498, https://doi.org/10.1039/C6TA07033G.
[50] N. Mileti´c, Z. Vukovi´c, A. Nastasovi´c, K. Loos, Macroporous poly (glycidylmethacrylate-co-ethylene glycol dimethacrylate) resins-versatile immobilization supports for biocatalysts, J. Mol. Catal. B Enzym 56 (2009) 196–201.

[51] W. Li, A. Zhang, H. Gao, M. Chen, A. Liu, H. Bai, L. Li, Massive preparation of pitch-based organic microporous polymers for gas storage, Chem. Commun. 52 (2016) 2780–2783, https://doi.org/10.1039/c5cc07908j.
[52] M. Mohammadi, Z. Habibi, S. Gandomkar, M. Yousefi, A novel approach for bioconjugation of Rhizomucor miehei lipase (RML) onto amine-functionalized supports; application for enantioselective resolution of rac-ibuprofen, Int. J. Biol. Macromol. 117 (2018) 523–531, https://doi.org/10.1016/j. ijbiomac.2018.05.218.
[53] J.C.S. Terra, A. Moores, Flavia C.C. Moura, Amine-functionalized mesoporous silica as a support for on-demand release of copper in the A3-coupling reaction: ultralow concentration catalysis and confinement effect, ACS Sustain. Chem. Eng. 7 (2019) 8696–8705, https://doi.org/10.1021/acssuschemeng.9b00576.
[54] J.N. Talbert, J.M. Goddard, Enzymes on material surfaces, Colloids Surf. B Biointerfaces 93 (2012) 8–19, https://doi.org/10.1016/j.colsurfb.2012.01.003.
[55] T. Jesionowski, J. Zdarta, B.J.A. Krajewska, Enzyme immobilization by adsorption: a review, Adsorption 20 (2014) 801–821, https://doi.org/10.1007/ s10450-014-9623-y.
[56] G. Gellf, J. Boudrant, Bed enzyme enzymes immobilized on a magnetic support preliminary study of a fluidized bed enzyme reactor, BBA 334 (1974) 467–470, https://doi.org/10.1016/0005-2744(74)90194-6.
[57] J. Del Arco, A.R. Alc´antara, R. Fern´andez-Lafuente, J. Fernandez-Lucas, Magnetic micro-macro biocatalysts applied to industrial bioprocesses, Bioresour. Technol. 322 (2021), 124547, https://doi.org/10.1016/j.biortech.2020.124547.
[58] Y. Amini, M. Shahedi, Z. Habibi, M. Yousefi, M. Ashjari, M. Mohammadi, A multi- component reaction for covalent immobilization of lipases on amine- functionalized magnetic nanoparticles: production of biodiesel from waste cooking oil, Bioresour. Bioprocess 9 (2022) 60, https://doi.org/10.1186/s40643-022-00552-0.
[59] M.R. Mehrasbi, J. Mohammadi, M. Peyda, M. Mohammadi, Covalent immobilization of Candida antarctica lipase on core-shell magnetic nanoparticles for production of biodiesel from waste cooking oil, Renew. Energy 101 (2017) 593–602, https://doi.org/10.1016/j.renene.2016.09.022.
[60] Y. Ren, J.G. Rivera, L. He, H. Kulkarni, D.-K. Lee, P.B. Messersmith, Facile, high efficiency immobilization of lipase enzyme on magnetic iron oxide nanoparticles via a biomimetic coating, BMC Biotechnol. 11 (2011) 63, https://doi.org/ 10.1186/1472-6750-11-63.
[61] M. Ashjaria, M. Garmroodi, F.A. Asl, M. Emampour, M. Yousefi, M.P. Lish, Z. Habibi, M. Mohammadi, Application of multi-component reaction for covalent immobilization of two lipases on aldehyde-functionalized magnetic nanoparticles; production of biodiesel from waste cooking oil, Process Biochem 90 (2020) 156–167, https://doi.org/10.1016/j.procbio.2019.11.002.
[62] Y. Jiang, C. Guo, H. Xia, I. Mahmood, C. Liu, H. Liu, Magnetic nanoparticles supported ionic liquids for lipase immobilization: enzyme activity in catalyzing esterification, Mol. Catal., B Enzym 58 (2009) 103–109, https://doi.org/ 10.1016/j.molcatb.2008.12.001.
[63] R. Castaldo, V. Ambrogi, R. Avolio, M. Cocca, G. Gentile, M.E. Errico, M. Avella, Functional hyper-crosslinked resins with tailored adsorption properties for environmental applications, Chem. Eng. J. 362 (2019) 497–503, https://doi.org/ 10.1016/j.cej.2019.01.054.
[64] R. Castaldo, G. Gentile, M. Avella, C. Carfagna, V. Ambrogi, Microporous hyper- crosslinked polystyrenes and nanocomposites with high adsorption properties: a review, Polymers 9 (2017) 651, https://doi.org/10.3390/polym9120651.
[65] R. Castaldo, R. Avolio, M. Cocca, G. Gentile, M.E. Errico, R. Avella, C. Carfagna, V. Ambrogi, A versatile synthetic approach toward hyper-cross-linked styrene- based polymers and nanocomposites, Macromolecules 50 (2017) 4132–4143, https://doi.org/10.1021/acs.macromol.7b00812.
[66] (a) J.L. Adrio, A.L. Demain, Microbial enzymes: Tools for biotechnological processes, Biomolecules 4 (2014) 117–139;
(b) F. Hasan, A.A. Shah, A. Hameed, Industrial applications of microbial lipases, Enzyme Microb. Technol. 39 (2006) 235–251.
[67] F. Hasan, A.A. Shah, A. Hameed, Industrial applications of microbial lipases, Enzym. Microb. Technol. 39 (2006) 235–251, https://doi.org/10.1016/j. enzmictec.2005.10.016.

[68] P. Domìnguez de Maria, J.M. Sanchez-Montero, J.V. Sinisterra, A.R. Alcantara, Understanding Candida rugosa lipases: an overview, Biotechnol. Adv. 24 (2006) 180–196, https://doi.org/10.1016/j.biotechadv.2005.09.003.
[69] W.C.A. Carvalho, J.H.H. Luiz, R. Fernandez-Lafuente, D.B. Hirata, A.A. Mendes, Eco-friendly production of trimethylolpropane triesters from refined and used soybean cooking oils using an immobilized low-cost lipase (Eversa>® Transform 2.0) as heterogeneous catalyst, Biomass-.-. Bioenerg. 155 (2021), 106302, https://doi.org/10.1016/j.biombioe.2021.106302.
[70] J. Barriuso, M.E. Vaquero, A. Prieto, M. Jesús Martínez, Structural traits and catalytic versatility of the lipases from the Candida rugosa-like family: a review, Biotechnol. Adv. 34 (2016) 874–885, https://doi.org/10.1016/j. biotechadv.2016.05.004.
[71] A. Bastida, P. Sabuquillo, P. Armisen, R. Fern´andez-Lafuente, J. Huguet, J.M. Guis´an, A single step purification, immobilization, and hyperactivation of lipases via interfacial adsorption on strongly hydrophobic supports, Biotechnol. Bioeng. 58 (1998) 486–493.
[72] E.A. Manoel, J.C.S. dos Santos, D.M.G. Freire, N. Rueda, R. Fernandez-Lafuente, Immobilization of lipases on hydrophobic supports involves the open form of the enzyme, Enzym. Microb. Technol. 71 (2015) 53–55.
[73] K. Wang, S. Sun, B. Ma, F. Dong, T. Huo, X. Li, Y. Zhao, H. Yu, Y. Huang, Construction and characterization of a nanostructured biocatalyst consisting of immobilized lipase on aminopropyl-functionalized montmorillonite, Appl. Clay Sci. 183 (2019), https://doi.org/10.1016/j.clay.2019.105329.
[74] B. Tural, S. Tural, E. Ertas¸, I˙. Yalınkılıç, A.S. Demir, Purification and covalent immobilization of benzaldehyde lyase with heterofunctional chelate-epoxy modified magnetic nanoparticles and its carboligation reactivity, J. Mol. Catal. B: Enzym 95 (2013) 41–47.
[75] F. Jamil, A.H.A. Muhtaseb, L.A. Haj, M.A.A. Hinai, P. Hellier, U. Rashid, Optimization of oil extraction from waste ‘‘Date pits” for biodiesel production, Energy Convers. Manag. 117 (2016) 264–272, https://doi.org/10.1016/j. enconman.2016.03.025.
[76] D.I. Hadaruga, N.G. Hadaruga˘, A. Hermenean, A. Riviș, V. Paˆslaru, G. Codina, Bionanomaterials: thermal stability of the oleic acid/a. - and b-cyclodextrin complexes, Rev. Chim. 59 (2008) 994–998.
[77] R. Castaldo, R. Avolio, M. Cocca, M.E. Errico, M. Avella, G. Gentile, Amino- functionalized hyper-crosslinked resins for enhanced adsorption of carbon dioxide and polar dyes, Chem. Eng. J. 418 (2021), 129463, https://doi.org/ 10.1016/j.cej.2021.129463.
[78] M. Feckova´, J. To´th, P. S˘´alek, A. S˘panov´a, D. Hor´ak, Q.T.H. Shubhra, A. Kova˘rík,
J. Gyenis, B. Rittich, Capture of DNAs by magnetic hypercrosslinked poly(styrene- co-divinylbenzene) microspheres, J. Mater. Sci. 56 (2021) 5817–5829, https:// doi.org/10.1007/s10853-020-05649-5.
[79] S. Tvorynska, J. Barek, B. Josypcuk, Influence of different covalent immobilization protocols on electroanalytical performance of laccase-based biosensors, Bioelectrochemistry 148 (2022), 108223.
[80] K.E. Wang, S. Sun, B. Ma, F. Dong, T. Huo, X. Li, Y. Huang, Construction and characterization of a nanostructured biocatalyst consisting of immobilized lipase on aminopropyl-functionalized montmorillonite, Appl. Clay Sci. 189 (2019), 105329, https://doi.org/10.1016/j.clay.2019.105329.
[81] B. Thangaraj, P. Raj Solomon, Immobilization of lipases - a review. Part I: enzyme immobilization, ChemBioEng Rev. 6 (2019) 157–166, https://doi.org/10.1002/ cben.201900016.
[82] S. Kumar, A.K. Jana, M. Maiti, I. Dhamija, Carbodiimide-mediated immobilization of serratiopeptidase on amino-, carboxyl-functionalized magnetic nanoparticles and characterization for target delivery, J. Nanopart. Res 16 (2014) 1–23, https://doi.org/10.1007/s11051-013-2233-x
[83] A. Cano, C. Minguillon, C. Palet, Immobilization of endo-1,4-bxylanase on polysulfone membranes acrylate: synthesis and characterization, J. Membr. Sci. 280 (2006) 383–388, https://doi.org/10.1016/j.memsci.2006.01.041.
[84] M. Bradford, A rapid and sensitive method for the quantitation of microgram quantities of protein utilizing the principle of protein-dye binding, J. Anal. Biochem. 72 (1976) 248–254.
[85] Y. Yong, Y.X. Bai, Y.F. Li, L. Lin, Y.J. Cui, C.G. Xia, Characterization of Candida rugosa lipase immobilized onto magnetic microspheres with hydrophilicity, Process Biochem. 43 (2008) 1179–118537.
[86] M.N. Gupta, Enzyme function in organic solvents, Eur. J. Biochem. 203 (1992) 25–32, https://doi.org/10.1111/j.1432-1033.1992.tb19823.x.

[87] A.B. Salleh, M. Basri, S.W. Tan, M.B. Abdul Rahman, K. Dzulkefly, R.N.Z. Rahman, C.N.A. Razak, Synthesis of fatty alkanolamides by using immobilized lipases, Malays, J. Anal. Sci. 7 (2001) 281–285.
[88] E.R. Gunawan, M. Basri, M.B.A. Rahman, A.B. Salleh, R.N.A. Rahman, lipase- catalyzed synthesis of palm based wax ester, J. Oleo Sci. 53 (2004) 471–477, https://doi.org/10.5650/jos.53.471.
[89] L.C.D. Lima, D.G.C. Peres, A.A. Mendes, Kinetic and thermodynamic studies on the enzymatic synthesis of wax ester catalyzed by lipase immobilized on glutaraldehyde-activated rice husk particles, Bioprocess Biosyst. Eng. 41 (2018) 991–1002, https://doi.org/10.1007/s00449-018-1929-9.
[90] A. Abdullah, S.S.A. Gani, T.Y.Y. Hin,Z.A. Haiyee, U.H. Zaidan, M.A. Kassimgh, M.I.E. Halmii, Lipase-catalyzed synthesis of red pitaya (Hylocereus polyrhizus) seed oil esters for cosmeceutical applications: process optimization using response surface methodology, RSC Adv. 9 (2019) 5599–5609, https://doi.org/10.1039/ C8RA09418G.
[91] M. Sarno, E. Ponticorvo, C. Cirillo, High surface area monodispersed Fe3O4 nanoparticles alone and on physical exfoliated graphite for improved supercapacitors, J. Phys. Chem. Solids 99 (2016) 138–147, https://doi.org/ 10.1016/j.jpcs.2016.08.019.
[92] S.H. Chaki, T.J. Malek, M.D. Chaudhary, J.P. Tailor, M.P. Deshpande, Magnetite Fe3O4 nanoparticles synthesis by wet chemical reduction and their characterization, Adv. Nat. Sci: Nanosci. Nanotechnol. 6 (2020), 035009, https:// doi.org/10.1016/j.heliyon.2020.e03784.
[93] M. Sarno, M. Iuliano, S. De Pasquale, E. Ponticorvo, A new nano-catalyst for sawdust hydrolysis, Appl. Catal. A 602 (2020), 117686, https://doi.org/10.1016/ j.apcata.2020.117686.
[94] W.M. Zhang, Q. Du, B.C. Pan, L. Lv, C.H. Hong, Z.M. Jiang, D.Y. Kong, Adsorption equilibrium and heat of phenol onto aminated polymeric resins from aqueous solution, Colloids Surf. A 346 (2009) 34–38, https://doi.org/10.1016/j. colsurfa.2009.05.022.
[95] W.L. Yang, X.C. Li, B.C. Pan, L. Lv, W.M. Zhang, Effective removal of effluent organic matter (EfOM) from bio-treated coking wastewater by a recyclable aminated hyper-cross-linked polymer, Water Res. 47 (2013) 4730–4738, https:// doi.org/10.1016/j.watres.2013.05.032.
[96] J. Wang, D. Yue, H. Wang, In situ Fe3O4 nanoparticles coating of polymers for separating hazardous PVC from microplastic mixtures, Chem. Eng. J. 407 (2021), 127170, https://doi.org/10.1016/j.cej.2020.127170.
[97] A. Natalello, D. Ami, S. Brocca, M. Lotti, S.M. Doglia, Secondary structure, conformational stability and glycosylation of a recombinant Candida rugosa lipase studied by fourier-transform infrared spectroscopy, Biochem. J. 385 (2005) 511–517, https://doi.org/10.1042/BJ20041296.
[98] M. Zhang, S. Sun, R. Lv, Y.A. Golubev, K. Wang, F. Dong, O.B. Kotova, E.
L. Kotova, Construction and characterization of a nanostructured biocatalyst consisting of immobilized lipase On Mg-amino-clay, Clays Clay Min. 69 (2021) 434–442, https://doi.org/10.1007/s42860-021-00130-z.
[99] J. Boudrant, J.M. Woodley, R. Fernandez-Lafuente, Parameters necessary to define an immobilized enzyme preparation, Process Biochem. 90 (2020) 66–80, https://doi.org/10.1016/j.procbio.2019.11.026.
[100] S. Ma, J. Mu, Y. Qu, L. Jiang, Effect of refluxed silver nanoparticles on inhibition and enhancement of enzymatic activity of glucose oxidase, Colloids Surf. A: Physicochem. Eng. Asp. 345 (2009) 101–105, https://doi.org/10.1016/j. colsurfa.2009.04.038.
[101] W. Tang, C. Chen, W. Sun, P. Wang, D. Wei, Low-cost mussel inspired poly (Catechol/Polyamine) modified magnetic nanoparticles as a versatile platform for enhanced activity of immobilized enzyme, Int. J. Biol. Macromol. 128 (2019) 814–824, https://doi.org/10.1016/j.ijbiomac.2019.01.161.
[102] K. Vasi´c, Z˘. Knez, M. Leitgeb, Immobilization of alcohol dehydrogenase from Saccharomyces cerevisiae onto carboxymethyl dextran-coated magnetic nanoparticles: a novel route for biocatalyst improvement via epoxy activation, Sci. Rep. 10 (2020) 19478, https://doi.org/10.1038/s41598-020-76463-x.
[103] S. Arana-Pen˜a, Y. Lokha, R. Ferna´ndez-Lafuente, Immobilization of eversa lipase on octyl agarose beads and preliminary characterization of stability and activity features, Catalysts 8 (2018) 511, https://doi.org/10.3390/catal8110511.
[104] M.L. Verma, W. Azmi, S.S. Kanwar, Synthesis of ethyl acetate employing celite- immobilized lipase of Bacillus cereus MTCC 8372, Acta Microbiol. Immunol. Hung. 56 (2009) 229–242, https://doi.org/10.1556/AMicr.56.2009.3.3.

[105] K.M.W. Syamsu, M.R. Salina, S.O. Siti, M.N. Hanina, M.A.R. Basyaruddin, K. Jusoff, Green synthesis of lauryl palmitate via lipase-catalyzed reaction, World Appl. Sci. J. 11 (2010) 401–407.
[106] Y. Bi, M. Yu, H. Zhou, H. Zhou, P. Wei, Biosynthesis of oleyl oleate in solvent-free system by Candida rugosa Lipase (CRL) immobilized in macroporous resin with cross-linking of aldehyde-dextran, J. Mol. Catal. B Enzym 133 (2016) 1–5, https://doi.org/10.1016/j.molcatb.2016.05.002.
[107] F. Kazenwadel, H. Wagner, B.E. Rapp, M. Franzreb, Optimization of enzyme immobilization on magnetic microparticles using 1-ethyl-3-(3- dimethylaminopropyl)carbodiimide (EDC) as a crosslinking agent, Anal. Methods 7 (2015) 10291, https://doi.org/10.1039/c5ay02670a.
[108] L. Deng, X. Wang, K. Nie, F. Wang, J. Liu, P. Wang, T. Tan, Synthesis of wax esters by lipase-catalyzed esterification with immobilized lipase from Candida sp. 99–125, Chin. J. Chem. Eng. 19 (2011) 978–982, https://doi.org/10.1016/ S1004-9541(11)60080-3.
[109] Y. Bi, M. Yu, H. Zhou, H. Zhou, P. Wei, Biosynthesis of oleyl oleate in solvent-free system by Candida rugosa Lipase (CRL) immobilized in macroporous resin with cross-linking of aldehyde-dextran, J. Mol. Catal. B: Enzym 133 (2016) 1–5, https://doi.org/10.1016/j.molcatb.2016.05.002.
[110] K.C. Badgujar, B.M. Bhanage, The combine use of ultrasound and lipase immobilized on co-polymer matrix for efficient biocatalytic application studies, J. Mol. Catal. B: Enzym 122 (2015) 255–264, https://doi.org/10.1016/j. molcatb.2015.09.012.
[111] N.R. Khan, S.V. Jadhav, V.K. Rathod, Lipase catalysed synthesis of cetyl oleate using ultrasound: optimisation and kinetic studies, Ultrason. Sonochem. 27 (2015) 522–529, https://doi.org/10.1016/j.ultsonch.2015.03.017.
[112] M.D. Alves, F.M. Aracri, E.C. Cren, A.A. Mendes, Isotherm, kinetic, mechanism and thermodynamic studies of adsorption of a microbial lipase on a mesoporous and hydrophobic resin, Chem. Eng. J. 311 (2017) 1–12, https://doi.org/10.1016/ j.cej.2016.11.069.
[113] P. Ungcharoenwiwat, A. Kittikun, Enzymatic synthesis of coconut oil based wax esters by immobilized lipase EQ3 and commercial lipozyme RMIM, Electron. J. Biotechnol. 47 (2020) 10–16, https://doi.org/10.1016/j.ejbt.2020.06.005.
[114] P. Ungcharoenwiwat, B. Canyuk, A. H-Kittikun, Synthesis of jatropha oil based wax esters using an immobilized lipase from burkholderia sp. EQ3 and lipozyme RM IM, Process Biochem 51 (2016) 392–398, https://doi.org/10.1016/j. procbio.2015.12.019.
[115] P.S. Keng, M. Basri, M.R.S. Zakaria, M.B.A. Rahman, A.B. Ariff, R.N.A. Rahman,
A.B. Salleh, Newly synthesized palm esters for cosmetics industry, Ind. Crop. Prod. 29 (2009) 37–44, https://doi.org/10.1016/j.indcrop.2008.04.002.

Fig. 1. Photo of waste fish and oil extracted from waste fish.

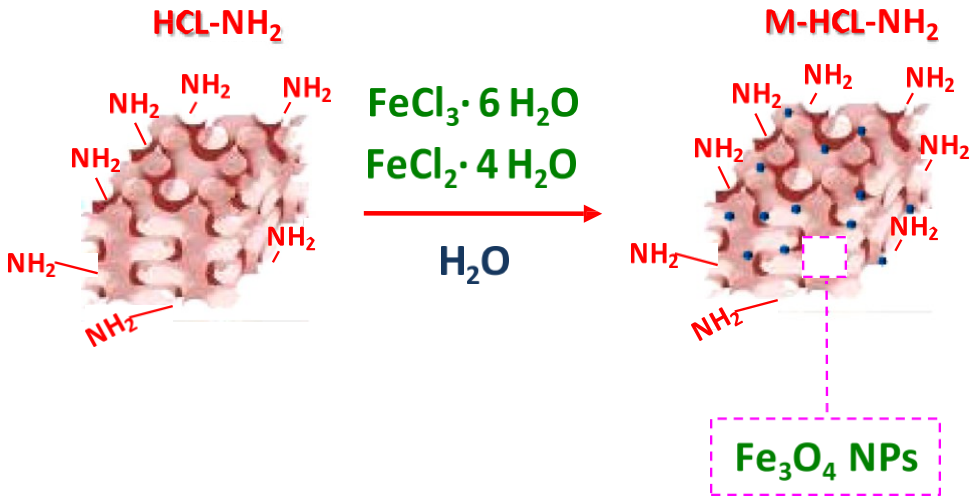

Fig. 2. Schematic illustration of precipitation of iron oxide nanoparticles (Fe_3O_4 NPs) in amino-functionalized hyper cross-linked resin (HCLR-NH_2).

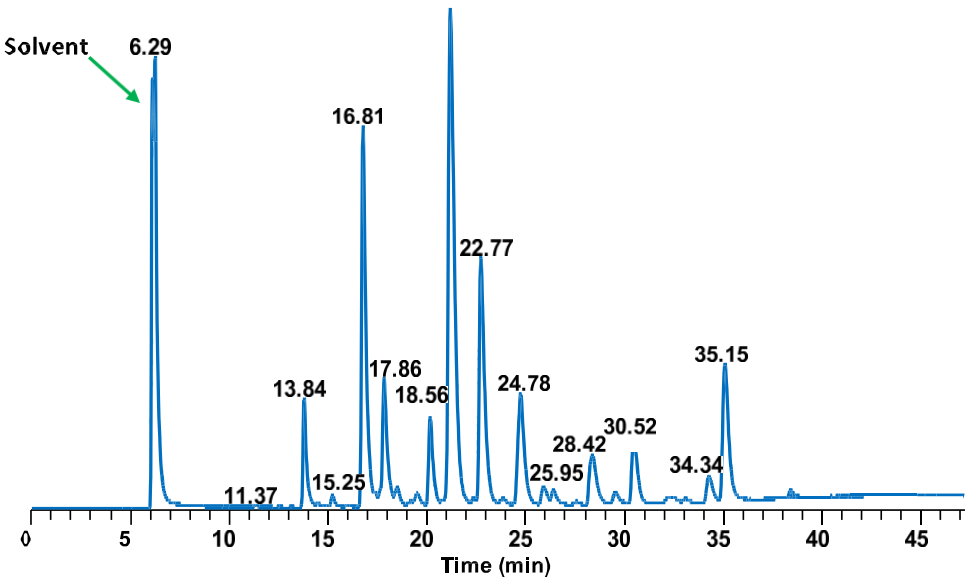

Fig. 3. *Gas chromatography* profile of extracted waste fish oil.

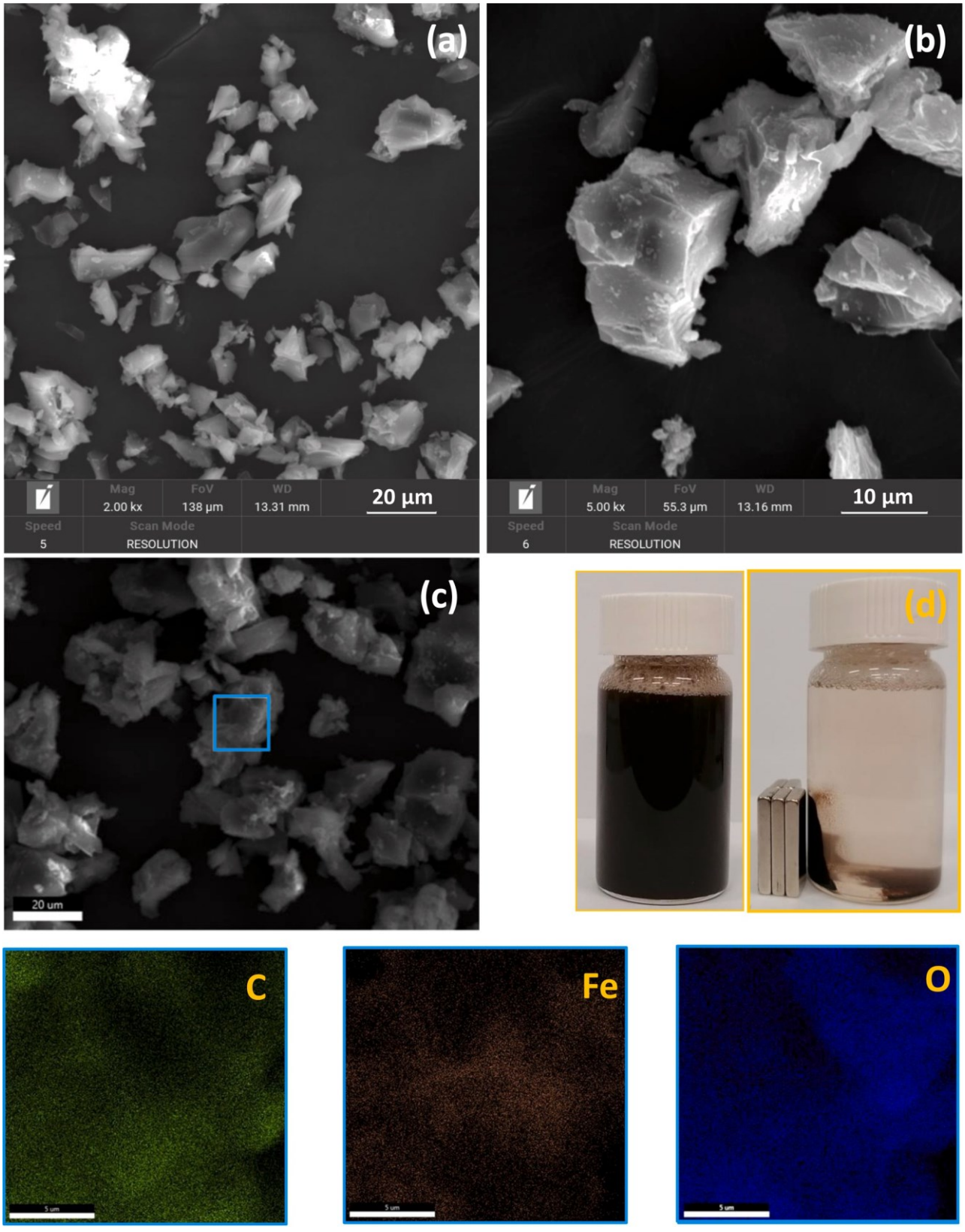

Fig. 4. a, b) Scanning electron microscopy (SEM) analysis of amino-functionalized hyper cross-linked resin (HCLR-NH_2) and magnetic amino-hyper cross-linked (M- HCLR-NH_2) resin; c) Energy-dispersive X-ray spectroscopy (EDX) elemental maps of magnetic amino-hyper cross-linked (M-HCLR-NH_2) for C, Fe, and O elements from the blue box; d) Photos of a M-HCLR-NH_2 resin solution.

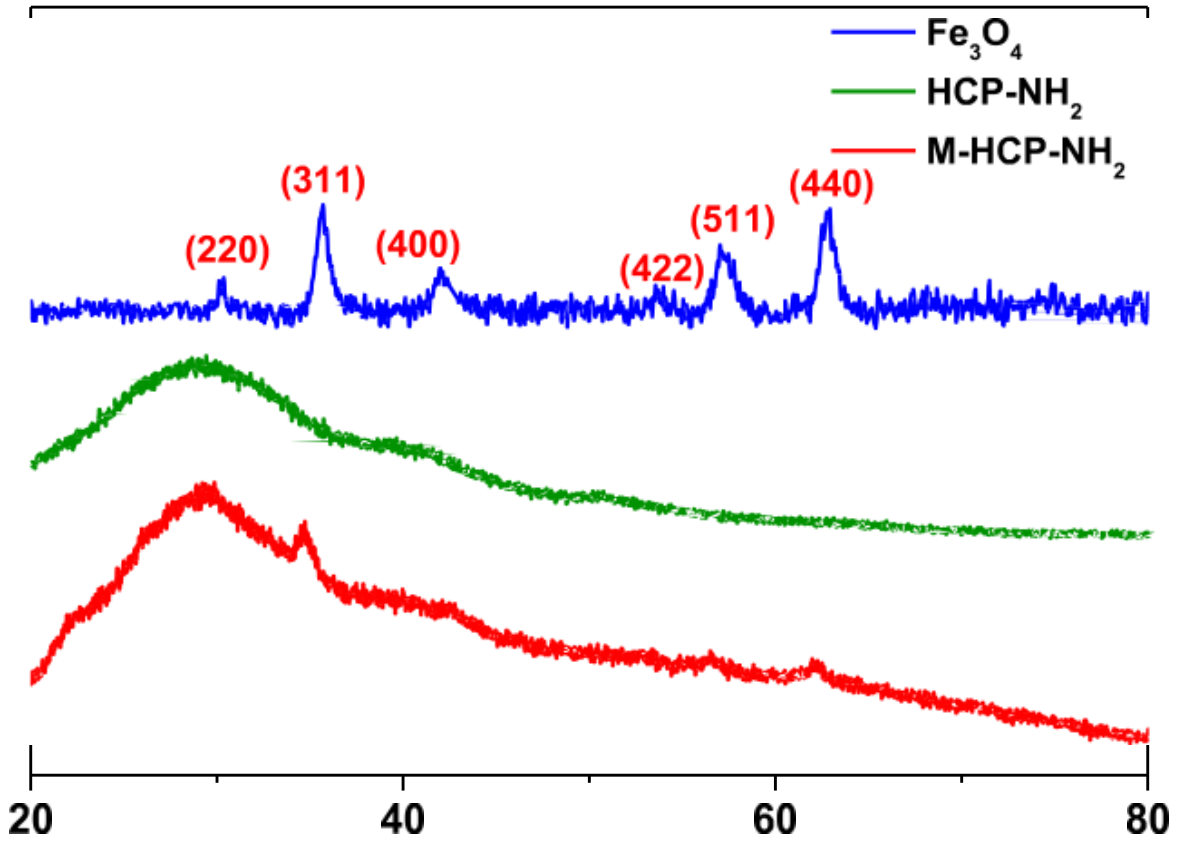

Fig. 5. X-Ray diffraction (XRD) profile of Fe_3O_4, amino-hyper cross-linked resin ($HCP\text{-}NH_2$) and magnetic amino-hyper cross-linked resin ($M\text{-}HCLR\text{-}NH_2$) in the range 20–80 2 Theta.

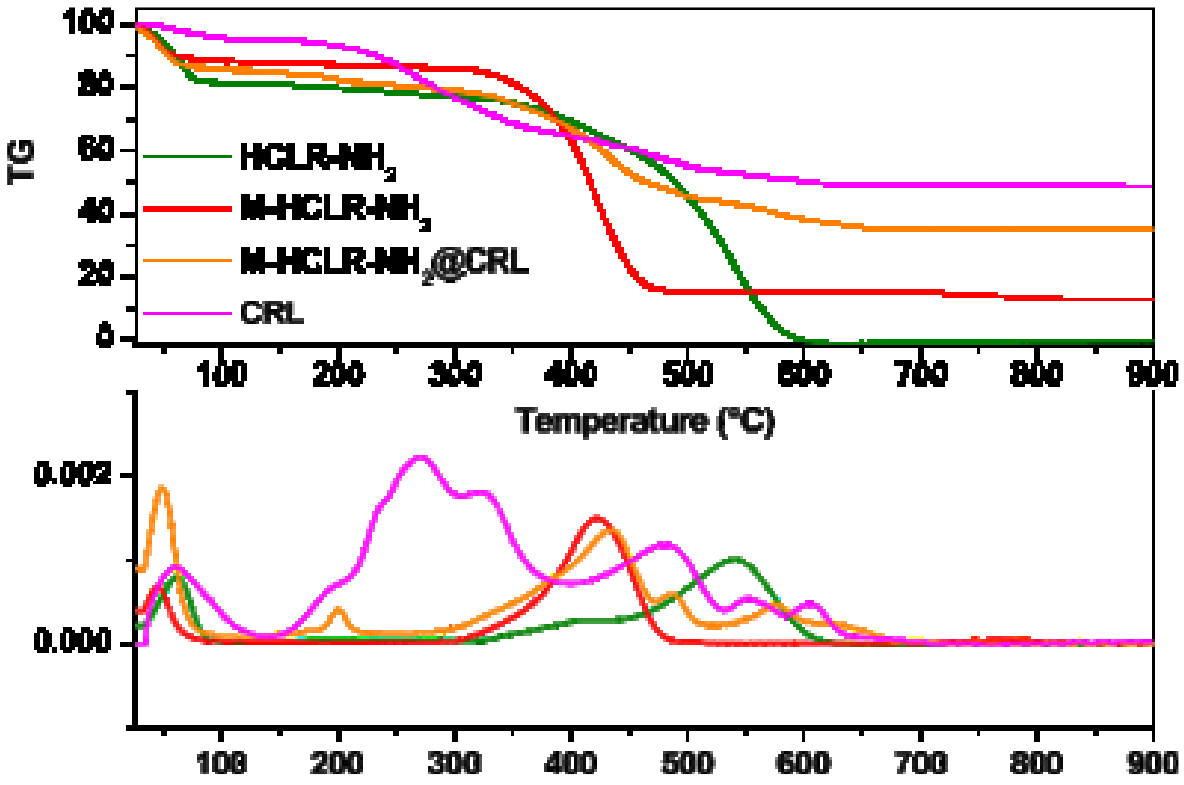

Fig. 6. Thermogravimetric analysis (TG-DTG) profiles of amino-functionalized hyper cross-linked resin ($HCLR\text{-}NH_2$), magnetic amino-hyper cross-linked resin ($M\text{-}HCLR\text{-}NH_2$), magnetic amino-hyper cross-linked resin after lipase immobi- lization ($M\text{-}HCLR\text{-}NH_2$ @CRL) and *Candida rugosa lipase* (Sigma Aldrich).

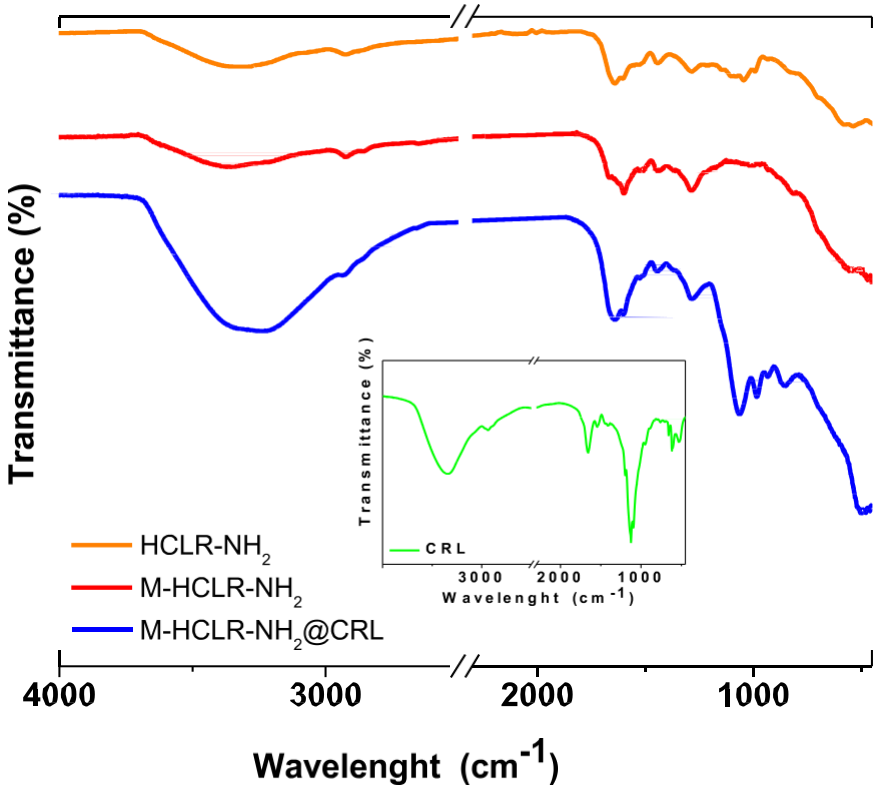

Fig. 7. Fourier-transform infrared spectra (FT-IR) spectra in the range of wavenumber 4000–500 cm^{-1} of amino-functionalized hyper cross-linked resin (HCLR-NH_2), magnetic amino-hyper cross-linked resin (M-HCLR-NH_2), magnetic amino-hyper cross-linked resin after lipase immobilization (M-HCLR-NH_2 @CRL), and *Candida rugosa lipase* (Sigma Aldrich, insert).

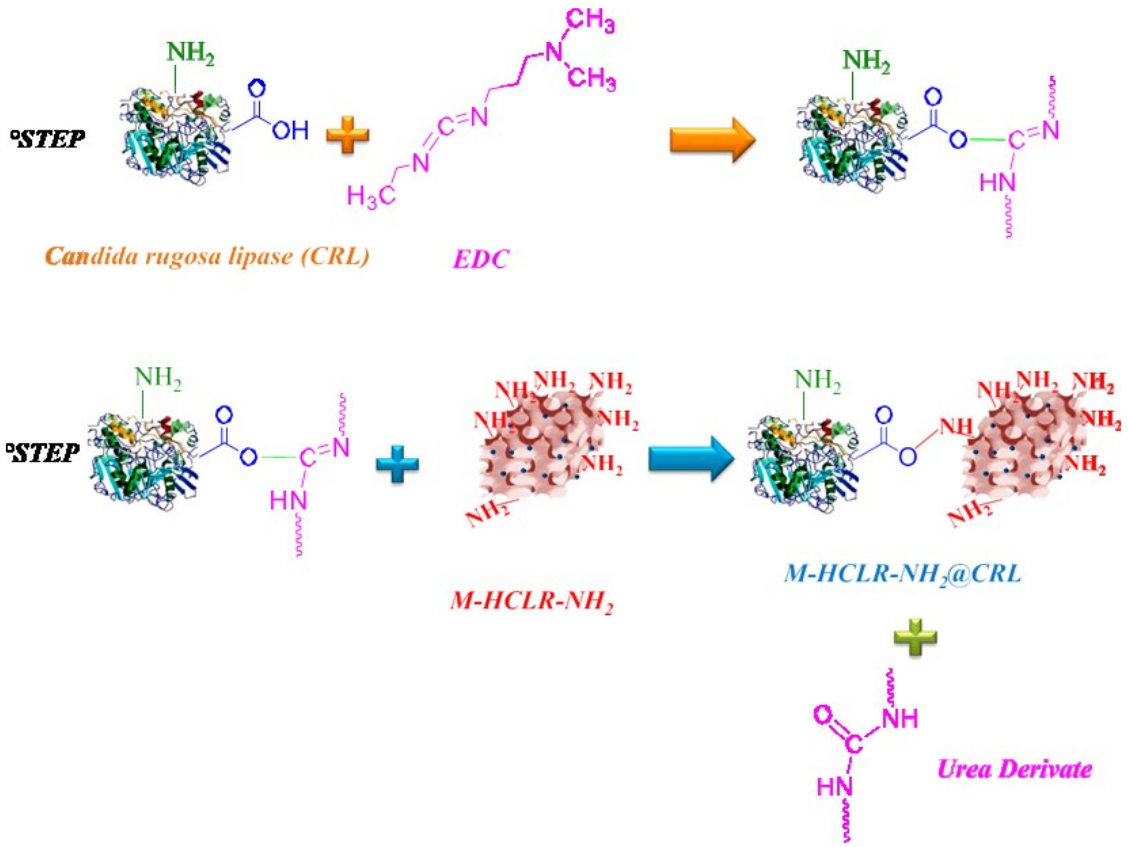

Fig. 8. Schematic illustration of 1-Ethyl-3-(3-dimethylaminopropyl) carbodiimide (EDC)-mediated enzyme immobilization on magnetic amino resin

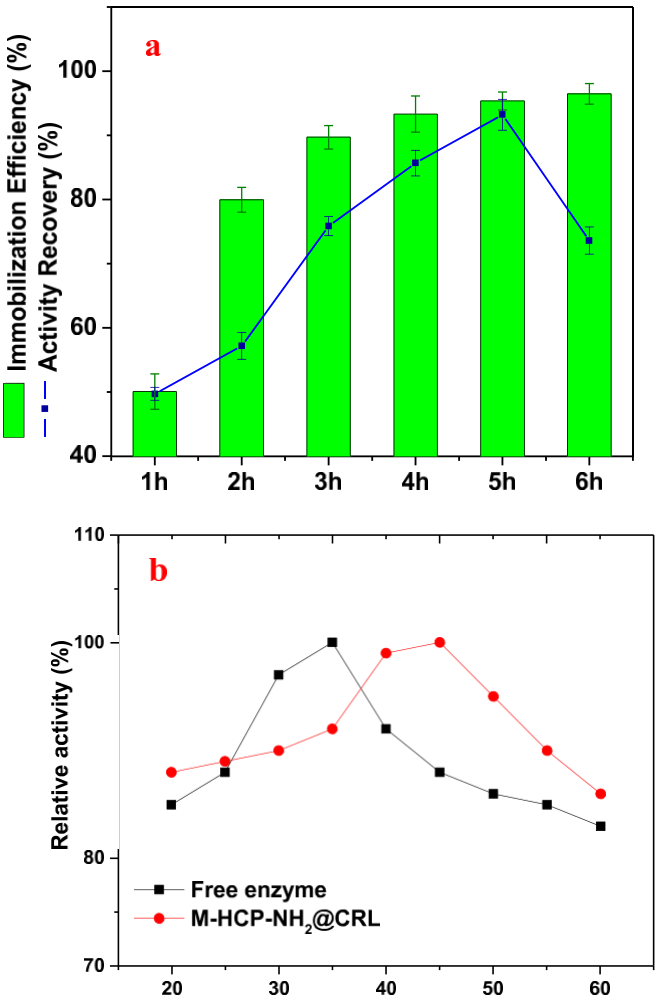

Fig. 9. Immobilization efficiency and activity recovery (a), Effect of coupling time. Immobilization conditions: coupling temperature, 4 ˚C; lipase concentration, 2.5 g/l; pH, 7; and, magnetic resin concentration, 5 mg/ml) All values are expressed as mean±standard deviation of two replicates; Effect of temper- ature on activities of the soluble and immobilized lipases (b). The maxima were defined as 100% activity. Immobilization conditions: coupling time, 5 h, coupling temperature, 4 ˚C; lipase concentration, 2.5 g/l; pH, 7; and, magnetic resin concentration, 5 mg/ml).

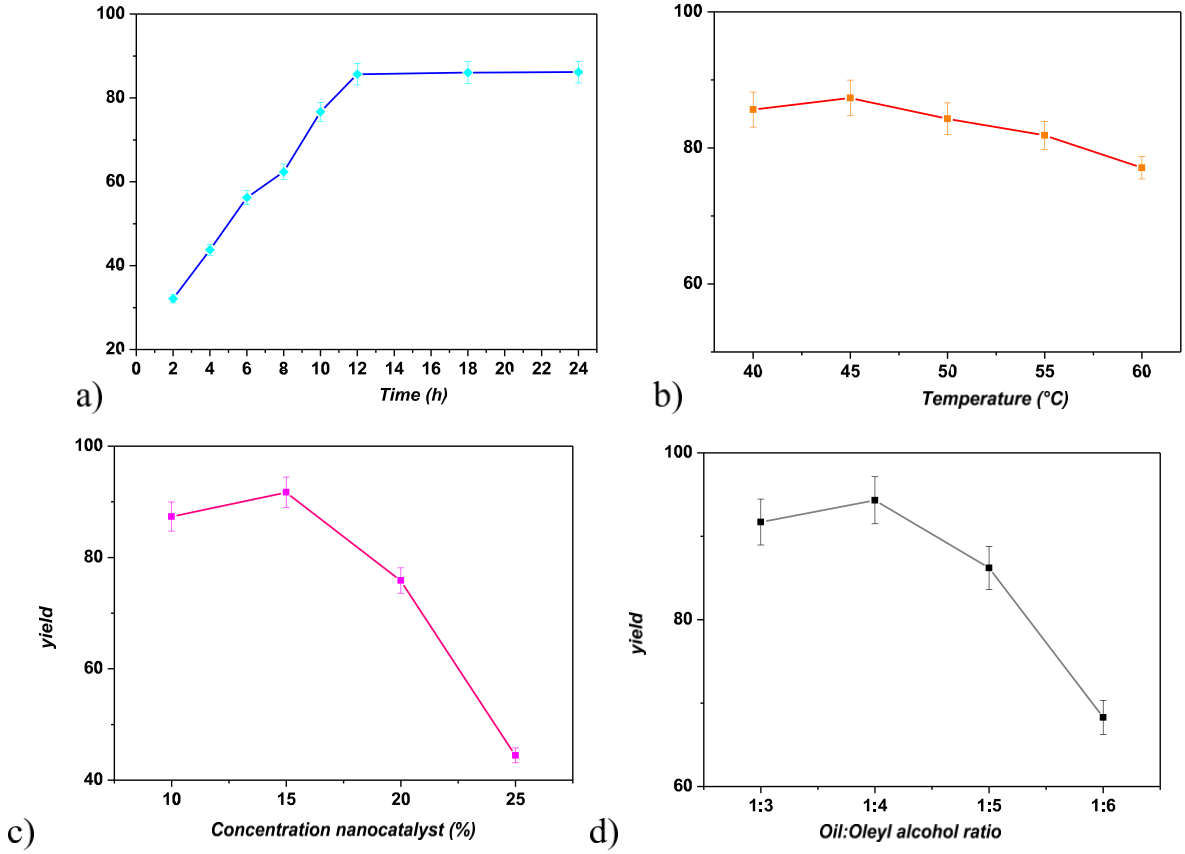

Fig. 10. a) Effect of the time during wax esters synthesis on M-HCLR-NH_2 @CRL (reaction conditions: temperature, 40 °C; immobilized enzyme concentration, 10%; oil:oleyl alcohol molar ratio 1:3 M); b) Effect of the reaction temperature during wax esters synthesis (reaction conditions: time, 12 h; immobilized enzyme concentration, 10 wt%; oil:oleyl alcohol molar ratio 1:3 M); c) Effect of the immobilized enzyme concentration during wax esters synthesis (reaction conditions: time, 12 h; temperature, 45 °C; oil:oleyl alcohol molar ratio 1:3 M); d) Effect of oil: oleyl alcohol ratio during wax esters synthesis (reaction conditions: time, 12 h; reaction temperature, 45 °C; and, immobilized enzyme concentration, 15%). All values are expressed as mean standard deviation of three replicates. Immobilization conditions: coupling time, 5 h, coupling temperature, 4 °C; lipase concentration, 2.5 g/l; pH, 7; and, magnetic resin concentration, 5 mg/ml).

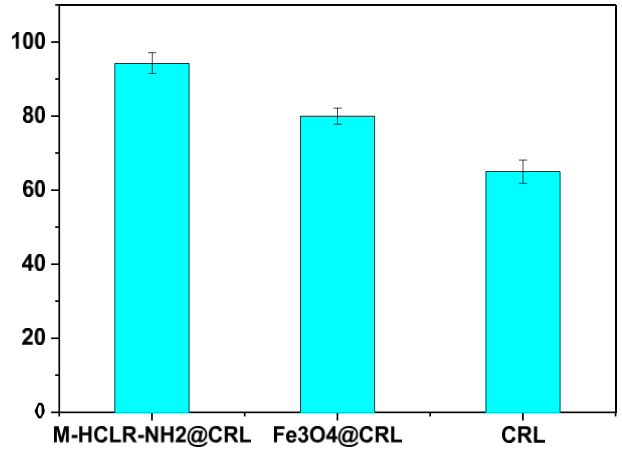

Fig. 11. Effect of the catalytic activity of M-HCLR-NH_2 @CRL, Fe_3O_4 @CRL, and free *Candida rugosa* lipase (CRL) on wax esters synthesis, see the experimental section for details. Reaction conditions: temperature, 45 °C; enzyme concentration, 15%; oil:oleyl alcohol molar ratio 1:4 M; and, time, 12 h. All values are expressed as mean standard deviation of three replicates. Immobi- lization conditions: coupling time, 5 h, coupling temperature, 4 °C; lipase concentration, 2.5 g/l; pH, 7; and, magnetic resin concentration, 5 mg/ml).

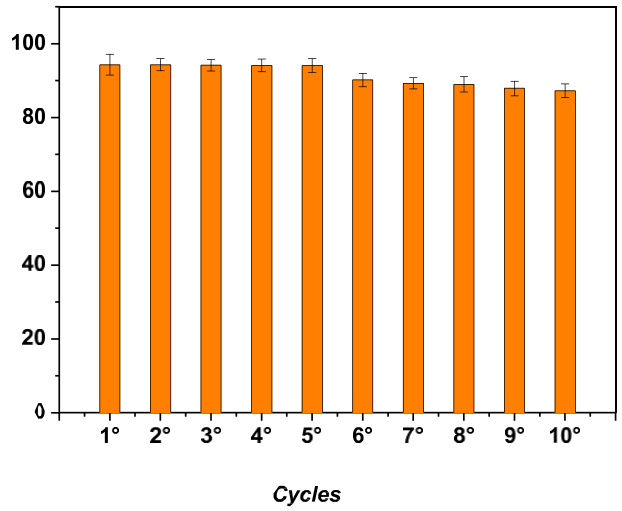

Fig. 12. Effect of cycles on wax esters synthesis; reaction conditions: time, 12 h; temperature, 45 °C; immobilized enzyme concentration, 15%; oil:oleyl alcohol molar ratio 1:4 M. All values are expressed as mean standard deviation of three replicates. Immobilization conditions: coupling time, 5 h, coupling temperature, 4 °C; lipase concentration, 2.5 g/l; pH, 7; and, magnetic resin concentration, 5 mg/ml).

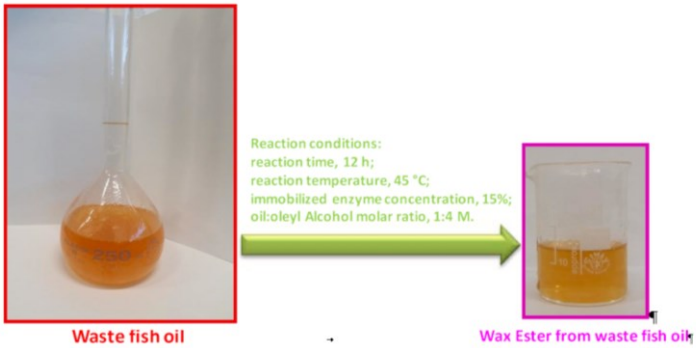

Fig. 13. Photos of waste fish oil and produced wax ester by immobilized *Candida rugosa* lipase (CRL).

Table 1
Fatty acids composition (% of total fatty acids) of the extracted waste fish oil.

Fatty acid	C number	RT (min)	wt. (%)[SEO]
Lauric acid	C12:0	11.37	0.07 ± 0.02
Tetradecanoic acid	C14:0	13.84	4.10 ± 2.0
Pentadecanoic acid	C15:0	15.25	0.40 ± 0.3
Palmitic acid	C16:0	16.81	16.64 ± 1.7
Palmitoleate acid	C16:1	17.86	6.13 ± 3.1
cis-10-Heptadecenoic acid	C17:1	18.56	0.88 ± 0.5
cis-9-Heptadecenoate acid	C17:1	19.55	0.69 ± 0.2
Stearic acid	C18:0	20.21	3.64 ± 2.0
Oleic acid	C18:1n9c	21.23	29.17 ± 3.4
Linoleic acid	C18:2n6c	22.77	12.87 ± 2.3
cis-11-Eicosanoic acid	C20:1n9c	24.78	6.91 ± 3.0
Linolenic acid	C18:3n6c	25.95	0.93 ± 0.9
Cis-11,14-Eicosanoic acid	C20:2	26.43	0.73 ± 0.4
Cis-11-Docosenoic acid	C22:1	28.42	3.53 ± 2.0
5,8,11,14,17- Eicosapentaenoic acid	C20:5n3	30.52	3.76 ± 2.1
7,10,13,16,19- Docosapentaenoic acid	C22:5	34.34	1.49 ± 1.3
4,7,10,13,16,19- Docosahexaenoic acid	C22:6n3	35.15	8.06 ± 1.0

All values are expressed as mean±standard deviation of three replicates. SEO= solvent extracted oil.

Table 2
Physico-chemical properties of waste fish oil.

Property	Value[SEO]
Acid value (mgKOH/g)	4.15 ± 1.29
Free fatty acid content (%)	2.08 ± 1.16
Moisture (%)	0.08 ± 0.06
Saponification Index (mgKOH/g)	176.68 ± 2.1
Iodine Value (gI_2/100 g oil)	125.5 ± 3.71

All values are expressed as mean±standard deviation of three replicates. SEO= solvent extracted oil.

Table 3
Literature survey for the enzymatic synthesis of wax esters by acid and oil.

Lipase source	Support	Immobilization	Reaction Conditions		Solvent	Reaction time (h)	Conversion (%)	Reusability run	Ref.
Candida sp. 99–125	Textile membrane	Physical adsorption	Esterification	T, 40 °C, molar ratio acid: alcohol of 1:0.9 10% m/m of biocatalyst	Solvent-free	24	95	7	[108]
Candida rugosa	Amino macroporous resin (LX-1000HA)	Physical adsorption		T, 40 °C molar ratio acid: alcohol of 1:1 10% m/m of biocatalyst	Solvent-free	12	92.6	8	[109]
	Amino macroporous resin (LX-1000HA) crosslinked with aldehyde dextran (6000 Da)	Covalent attachment						8	
Bacillus stearothermophilus MC7	Nanosized tin dioxide (nanoSnO_2)	Physical adsorption		T, 65 °C molar ratio acid: alcohol of 1:1 7.2% m/m of biocatalyst,	Solvent-free	5	75	8	[110]
					Ionic liquid [OMIM][Cl]	5	95	8	
Lipase B from *Candida antarctica*	Polyacrylate beads	Covalent attachment		T, 60 °C molar ratio acid:alcohol of 1:2 5% of biocatalyst	Solvent-free	0.5	95.96	7	[110]
Thermomyces lanuginosus	Poly-(styrene-divinylbenzene) resin	Physical adsorption		T, 50 °C molar ratio acid:alcohol of 1:1 15% m/m of biocatalyst	Solvent-free	0.5	90.5	5	[111]
				T, 45 °C molar ratio acid:alcohol of 1:1.25 7.5% m/m of biocatalyst	Heptane		92.5	8	[111]
Burkholderia sp. EQ3	Macroporous polypropylene-based hydrophobic porous support	Physical adsorption	Transesterification	T, 45 °C molar ratio oil: alcohol of 1:3 10 U enzyme	Isooctane	12	88.35	5	[112]
Burkholderia sp. EQ3	Polypropylene (Accurel MP–100)	Physical adsorption		T, 30 °C molar ratio oil: alcohol of 1:4 10 U enzyme	Isooctane	12	89	5	[113]
Rhizomucor miehei	Anionic resin (Duolite A568)				Hexane	12	86	5	[114]
Candida rugosa	M-HCLR-NH_2	Covalent attachment		T, 45 °C molar ratio oil: alcohol of 1:4 15% m/m of biocatalyst.	Hexane	12	94	10	This study

Table 4
Physico-chemical properties of ester from waste fish oil.

Property	Waste fish oil	Ester from waste fish oil
Acid value (mgKOH/g)	4.15 ± 1.29	< 1
Saponification Index (mgKOH/g)	176.68 ± 2.1	50.64 ± 3.2
Specific gravity	0.850 ± 1.3	0.823 ± 1.5
Iodine Value (gI_2/100 g oil)	125.5 ± 3.71	130.1 ± 1.8

All values are expressed as mean±standard deviation of three replicates.